Janus-Pro-R1: Advancing Collaborative Visual Comprehension and Generation via Reinforcement Learning

Kaihang Pan^{1,*}, Yang Wu^{2,*}, Wendong Bu^{1,*}, Kai Shen^{1,‡}, Juncheng Li^{1}, Yingting Wang^{2}, Yunfei Li^{2}, Siliang Tang^{1,†}, Jun Xiao^{1}, Fei Wu^{1}, Hang Zhao^{2}, Yueting Zhuang^{1}

Zhejiang University^{1}, Ant Group^{2}
{kaihangpan, wendongbu, shenkai, junchengli, siliang}@zju.edu.cn

Abstract

Recent endeavors in Multimodal Large Language Models (MLLMs) aim to unify visual comprehension and generation. However, these two capabilities remain largely independent, as if they are two separate functions encapsulated within the same model. Consequently, visual comprehension does not enhance visual generation, and the reasoning mechanisms of LLMs have not been fully integrated to revolutionize image generation. In this paper, we propose to enable the collaborative co-evolution of visual comprehension and generation, advancing image generation into an iterative introspective process. We introduce a two-stage training approach: supervised fine-tuning teaches the MLLM with the foundational ability to generate genuine CoT for visual generation, while reinforcement learning activates its full potential via an exploration-exploitation trade-off. Ultimately, we unlock the Aha moment in visual generation, advancing MLLMs from text-to-image tasks to unified image generation. Extensive experiments demonstrate that our model not only excels in text-to-image generation and image editing, but also functions as a superior image semantic evaluator with enhanced visual comprehension capabilities. Project Page: `https://janus-pro-r1.github.io`.

1 Introduction

Recently, multimodal large language models (MLLMs) [5, 12] have emerged to unify comprehension and generation across various modalities within the same next-token prediction paradigm of large language models (LLMs) [33]. Specifically, given a user query about comprehension—“What kind of dog is in this picture [IMG]”, or generation—“Generate an image of a cute cat”, the model can complete the task by sequentially predicting the appropriate text or image tokens.

However, for current MLLMs, visual comprehension and generation remain largely independent rather than forming a synergistic relationship, integrated into a single model seemingly just for the sake of avoiding parameter redundancy [5, 40, 51]. Especially in visual generation tasks, auto-regression-based methods are intended to unleash the powerful reasoning capabilities of MLLMs to infer more semantic-aligned images in more complex contexts. Unfortunately, even state-of-the-art MLLMs like Janus-Pro [5], still fall short of user expectations for basic text-to-image generation, also limited to accepting only pure text input for generation. This highlights that the robust reasoning mechanisms of LLMs have not been fully integrated to revolutionize, or even advance visual generation. Thus,

[*] Equal Contribution.
[‡] Project Leader.
[†] Corresponding Author.

39th Conference on Neural Information Processing Systems (NeurIPS 2025).

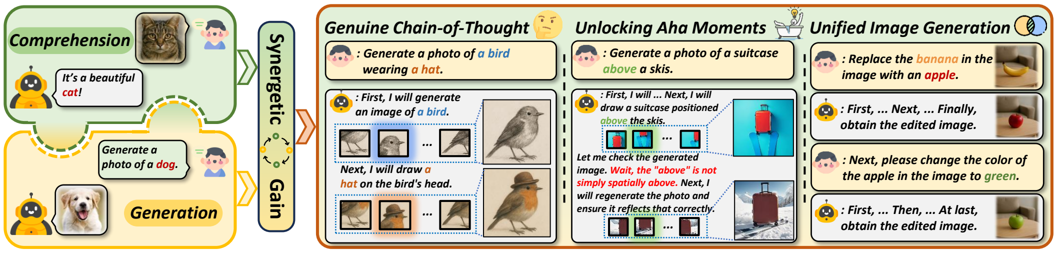
Comprehension
It's a beautiful cat!
Generate a photo of a dog.
Generation
Synergetic Gain
Genuine Chain-of-Thought
: Generate a photo of a bird wearing a hat.
: First, I will generate an image of a bird.
...
Next, I will draw a hat on the bird's head.
...
Unlocking Aha Moments
: Generate a photo of a suitcase above a skis.
: First, I will ... Next, I will draw a suitcase positioned above the skis.
...
Let me check the generated image. Wait, the "above" is not simply spatially above. Next, I will regenerate the photo and ensure it reflects that correctly.
...
Unified Image Generation
: Replace the banana in the image with an apple.
: First, ... Next, ... Finally, obtain the edited image.
: Next, please change the color of the apple in the image to green.
: First, ... Then, ... At last, obtain the edited image.

Figure 1: We could bring about three revolutionary benefits for image generation after collaborating the visual comprehension and generation capabilities with MLLMs.

a key question naturally arises: ***Is it feasible to synergize visual comprehension and generation, incorporating the reasoning mechanisms into visual generation?*** Once such collaboration is achieved, the MLLM can seamlessly combine and switch between its comprehension and generation capabilities, bringing about three revolutionary benefits for image generation, as shown in Figure 1.

1) Genuine Chain-of-Thought (CoT) [54]: A genuine CoT in MLLMs should be self-driven by the model's deep thinking within a unified next-token prediction framework based on the causal dependency of tokens. The visual comprehension and generation capabilities are naturally linked to form an interleaved text-image reasoning chain under the spontaneous scheduling of the MLLM, which can be treated as a CoT that truly helps produce more refined images.

2) Unlocking Aha Moments [16]: Genuine self-driven CoT further endows MLLMs with the ability of self-correction, unlocking the Aha Moments. After generating the initial image, the MLLM leverages its comprehension capability to reflect on the current generation. Once errors are detected, it re-engages its visual generation capabilities to re-produce images that better meet user requirements.

3) Enabling Unified Image Generation: The emergence of the above two benefits signifies that the model can effectively collaborate its visual comprehension and generative abilities. This not only enhances its performance in text-to-image tasks, but also enables flexible unified image generation [56] for any complex situational purposes, such as image editing.

Furthermore, the collaboration between visual comprehension and generation should yield **mutual benefits**. This means that as visual comprehension evolves the capabilities of visual generation, it also enhances its own performance in the process.

Motivated by the above goals, we develop Janus-Pro-R1, advancing text-to-image generation into an introspective process and taking a step toward unified image generation with the collaborative co-evolution of visual comprehension and generation capabilities. The visual generation capability anchors the lower bound, ensuring the model can produce appropriate images. Meanwhile, the visual comprehension capability elevates the upper bound, enabling robust reasoning chains that unlock Aha Moments in image generation.

Specifically, our training process comprises two stages. **In the first stage**, we employ supervised fine-tuning (**SFT**) to endow MLLMs with the foundational ability to construct a genuine reasoning chain for visual generation that triggers Aha moments. To achieve this, we break down the CoT generation into several sub-skills with a mixed training approach, upgrading text-to-image generation into an iterative introspection mechanism. After each round of generation, the MLLM self-reflects on whether the generated image meets the requirements and repeats the generation if it does not. The model's spontaneous self-reflection during this process forms genuine CoT for visual generation, triggering Aha Moments where the model redirects its reasoning back onto the correct path.

However, training solely based on SFT tends to naively mimic the training distribution rather than performing true reasoning. Therefore, **in the second stage**, we treat image generation as a long token-level Markov decision process and perform reinforcement learning (**RL**) based on GRPO algorithm [45]. Without any ground-truth images, we encourage the model to spontaneously collaborate its comprehension and generation capabilities for introspective text-to-image generation, also designing a bi-level QA-based reward function for optimization. It represents a trade-off between exploration and exploitation [48]: we avoid explicitly teaching the model how to solve the problem but encourage autonomous exploration, while we still provide it with appropriate incentives to facilitate effective exploitation. And we find that RL enables the MLLM to autonomously develop advanced CoT for image generation, evolving from initial imitation to genuine reasoning.

Thanks to the above training strategy, with Janus-Pro as the backbone, Janus-Pro-R1 achieves stronger text-to-image performance on various T2I benchmarks with the collaboration between the visual comprehension and generation capabilities. More remarkably, the capability synergy endows the MLLM with the potential for unified image generation tasks (*e.g.*, image editing) and further enhances its role as an excellent image semantic evaluator, bolstering its visual comprehension capabilities. Our main contributions are threefold:

- We introduce a two-stage training paradigm, collaborating the visual comprehension and generation capabilities within the MLLM to construct a genuine chain-of-thought and unlock the aha moments for text-to-image generation.
- We further extend text-to-image generation to the scenarios of image editing, unleashing the potential for unified image generation.
- Our model achieves superior performance on both text-to-image generation and image editing tasks, also possessing enhanced image comprehension capabilities.

2 Related Work

Unified Visual Comprehension and Generation. Recent studies focus on unifying visual comprehension and generation within a unified MLLM. Some efforts [12, 47, 50] cascade external diffusion models after the output of MLLMs for visual generation, while some approaches [5, 39, 64, 52, 35] tokenize images into a discrete space and then conducte unified AR for text and vision. Others [58, 63] try to integrate the objective of AR and diffusion into a single model. However, visual comprehension and generation still remain largely independent without collaborative synergy, and the strong reasoning mechanism of LLMs fails to revolutionize visual generation. In this paper, we aim to promote collaboration between these two capabilities, enabling a genuine CoT for visual generation and unlocking its Aha moments.

CoT in Visual Generation. Recently, some studies have attempted to introduce CoT into visual generation. [17] considers the CoT as intermediate images within the DDPM process. [10] proposes a combination of two models: MLLM for reasoning chain generation while the diffusion model interprets the CoT for image generation. Moreover, although [53] and the concurrent work [21] integrate the CoT and image generation within a single model, the CoT is more akin to a forced textual planning of the organization logic for the target image. This represents a rudimentary form of thinking, failing to genuinely drive the MLLM's deep reasoning and introspection for image generation. We argue that a true CoT should emerge spontaneously from the model's deep thinking, naturally collaborating its visual comprehension and generation capabilities into an interleaved image-text reasoning chain, which could unlock the Aha moment in visual generation.

3 Method

In this section, we introduce how to collaborate visual comprehension and generation abilities to achieve introspective image generation with genuine CoT that unlocks the Aha moments. We outline two training stages (Figure 2): supervised fine-tuning (§ 3.1) and reinforcement learning (§ 3.2). Finally, we further endow MLLMs with advanced capabilities of unified image generation (§ 3.3).

3.1 Supervised Fine-Tuning

Similar to teaching complex tasks in everyday scenarios, during the SFT phase, we break down the Chain of visual generation reasoning into several subtasks with a mixed training approach. By doing so, the MLLM acquires a preliminary ability to continuously imitate specific subtasks based on the current context, finally exploring a coherent reasoning chain for visual generation.

Data Preparation. We aim to construct an image-text collection $\mathcal{C} = \{\mathcal{P}_i : \{(\mathcal{I}_i^j, \mathcal{S}_i^j, \mathcal{R}_i^j)\}_{j=1}^M\}_{i=1}^N$ as the supervised training data, where each prompt $\mathcal{P}$ corresponds to M images $\mathcal{I}$. For each image-text pair, there is an associated semantic consistency score $\mathcal{S} \in [0, 1]$ and a detailed reason $\mathcal{R}$ for semantic matching ($\mathcal{S} > 0.5$) or non-matching ($\mathcal{S} < 0.5$), where $S^0 > S^1 > ... > S^M$.

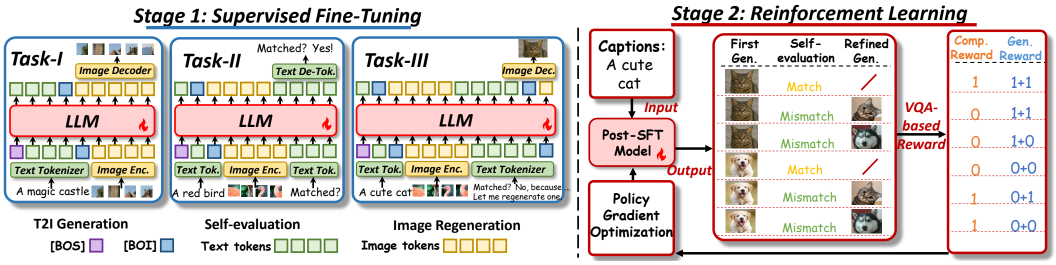

Figure 2: We include two training stages to unlock aha moments with CoT in visual generation: supervised fine-tuning and reinforcement learning.

Specifically, we first leverage the Qwen model [1] to develop a total of $N = 200,000$ prompts. For each prompt, we employ the FLUX [23] & Janus-Pro [5] for text-to-image generation, and then utilize the InternVL2.5-26B model [6] to evaluate whether the generated image and text are semantically consistent. We record the probability to answer "Yes" as P_{Yes} and "No" as P_{No}, with consistency score $\mathcal{S} = P_{\text{Yes}}/(P_{\text{Yes}} + P_{\text{No}})$. More details are shown in Appendix B.

Mixed Training. We first decompose the process of visual generation CoT, which elicits the aha moment, into three steps and designed three basic sub-tasks:

Task-I: Text-to-Image Generation: In $\mathcal{C}$, we select text-image pairs with $\mathcal{S} \geq 0.8$ for text-to-image training. The objective function is $p(y^{\mathcal{I}}) = \sum_{j=1}^{S^{\mathcal{I}}} \log P_\theta(y_j|y_{<j}, \mathcal{P})$, where $y^{\mathcal{I}}$ are tokens of a ground-truth image with sequence length as $S^{\mathcal{I}}$.

Task-II: Self-evaluation of Text-Image Consistency: We aim to enhance the capability of MLLM to determine whether given images are semantically consistent with the text, also providing the rationale for its judgment. To construct training data, for each prompt we first select $(t-1)$ images $\{\mathcal{I}^j, \mathcal{R}^j\}_{j=1}^{t-1}$ with $\mathcal{S} < 0.5$ as the preceding context ($t \geq 1$). Subsequently, we randomly select one positive image ($\mathcal{S} \geq 0.7$) and one negative image ($\mathcal{S} < 0.5$), respectively, as the target image $\mathcal{I}_t$ to be evaluated. The objective function is $p(y^{\mathcal{T}^t}) = \sum_{j=1}^{S^{\mathcal{T}^t}} \log P_\theta(y_j^{\mathcal{T}^t}|y_{<j}^{\mathcal{T}^t}, \mathcal{P}, \{\mathcal{I}^k, \texttt{No}, \mathcal{R}^k\}_{k=1}^{t-1}, \mathcal{I}^t)$, where $\mathcal{T}^t$ is $(\text{Yes}, \mathcal{R}^t)$ for positive images and $(\text{No}, \mathcal{R}^t)$ for negative images.

Task-III: Image Regeneration: We aim to enhance the MLLM to correct previous errors and regenerate accurate images. For each prompt, we first select t images $\{\mathcal{I}_j, \mathcal{R}_j\}_{j=1}^{t}$ with $\mathcal{S} < 0.5$ as the preceding context to simulate previous incorrect generations and corresponding self-reflections. Then we randomly select an image with $\mathcal{S} \geq 0.8$ as the ground-truth t-th regenerated image. The objective function is $p(y^{\mathcal{I}^{t+1}}) = \sum_{j=1}^{S^{\mathcal{I}}} \log P_\theta(y_j^{\mathcal{I}^{t+1}}|y_{<j}^{\mathcal{I}^{t+1}}, \mathcal{P}, \{\mathcal{I}^k, \texttt{No}, \mathcal{R}^k\}_{k=1}^{t})$.

Through the above supervised mixed training, the MLLM learns to integrate different subtasks for introspective text-to-image generation, developing a reasoning chain of deep thinking. Ultimately, it acquires the fundamental capability to trigger Aha moments.

3.2 Reinforcement Learning

The RL phase aims to effectively balance the exploration–exploitation trade-off to unlock the full potential of the MLLM. While encouraging the model to autonomously explore reasoning pathways, we also provide appropriate incentives for both its process of visual generation and comprehension as the exploitation, advancing it from mere imitation to genuine reasoning.

Bi-Level QA-based Rewards. The overall design philosophy of our reward model is to leverage QA-based visual comprehension models (*i.e.*, InternVL2.5-26B), which will return a consistency score $\texttt{R}^{QA}(\cdot) \in [0, 1]$ for each text-image pair, to assess the accuracy of the generated image and the MLLM's self-evaluation. And we provide incentives for the final output images along with their preceding reasoning chains, incorporating **bi-level reward scores**: visual generation reward $\texttt{R}^{Gen}$ and visual comprehension reward $\texttt{R}^{Comp}$. Assume that we permit the MLLM to perform up to a maximum of T-round image generations and the MLLM determines that it has correctly generated the image in the K-th round (resulting in a total of K images $\{\mathcal{I}^i\}_{i=1}^{K}$, $T \geq K$), we have:

(1) The generation reward $\mathtt{R}^{Gen} = \sum_{i=1}^{K-1} \mathtt{R}^{QA}(\mathcal{I}^i) + (T - K + 1) \times \mathtt{R}^{QA}(\mathcal{I}^K)$. The K-th image is assigned a potentially larger weight because it represents the final output with higher importance.

(2) The comprehension reward $\mathtt{R}^{Comp} = \sum_{i=1}^{K} \big(\mathbf{1} - |\mathtt{R}^{QA}(\mathcal{I}^i) - \mathtt{SE}(\mathcal{I}^i)|\big) \times T/K$, where $\mathtt{SE}(\mathcal{I}) = 0$ or 1 is the self-assessment on whether the generated image is semantically aligned with the text.

Policy Gradient. We leverage Group Relative Policy Optimization (GRPO) [45] as the training algorithm, which has been proven to be highly effective for exploring the reasoning capability of the LLMs. The preliminary of GRPO is given in Appendix A. Specifically, given the input prompt $\mathcal{P}$, we prompt the old policy π_{old} to first sample a group of G individual initial images $\{\mathcal{I}_i^1\}_{i=1}^G$ and obtain the first-round generation reward for each generated image $\{\mathtt{R}_{i,1}^{Gen}\}_{i=1}^G = \{\mathtt{R}^{QA}(\mathcal{I}_i^1)\}_{i=1}^G$. Subsequently, the MLLM will assess the semantic consistency between $\{\mathcal{I}_i^1\}_{i=1}^G$ and $\mathcal{P}$, returning the evaluation results as $\{\mathtt{SE}(\mathcal{I}_i^1)\}_{i=1}^G$. Based on the self-evaluation results, we further obtain the first-round comprehension rewards as $\{\mathtt{R}_{i,1}^{Comp}\}_{i=1}^G = \{\mathbf{1} - |\mathtt{R}^{QA}(\mathcal{I}_i^1) - \mathtt{SE}(\mathcal{I}_i^1)|\}_{i=1}^G$.

If the MLLM self-assesses that any generated image is not semantically aligned, it will initiate the next round for image regeneration and re-evaluation. Otherwise, it will directly output the image generated in the current round. Assuming that we conduct a maximum of T rounds in a group with the i-th sample undergoing K_i rounds, the final reward can be calculated as $\mathtt{R}_i = \mathtt{R}_i^{Gen} + \mathtt{R}_i^{Comp} = \big(\sum_{j=1}^{K_i-1} \mathtt{R}_{i,j}^{Gen} + (T - K_i) \times \mathtt{R}_{i,K_i}^{Gen}\big) + \sum_{j=1}^{K_i} \mathtt{R}_{i,j}^{Comp} \times T/K_i$. Then we can obtain the advantages $\{A_i\}$, where each A measures the relative quality of output compared to the average reward:

$$A_i = \frac{\mathtt{R}_i - \text{mean}\big(\{\mathtt{R}_i\}_{i=1}^G\big)}{\text{std}\big(\{\mathtt{R}_i\}_{i=1}^G\big)} \tag{1}$$

Finally, we upgrade the policy network parameters by the following training loss:

$$\mathcal{J}(\theta) = \mathbb{E}_{\substack{(\mathcal{P},a)\sim\mathcal{D} \\ \{y_i\}_{i=1}^G \sim \pi_{\theta_{\text{old}}}(\cdot|\mathcal{P})}} \left[\frac{1}{\sum_{i=1}^G |y_i|} \sum_{i=1}^{G} \sum_{j=1}^{|y_i|} \left(\min\Big(\rho_{i,j} A_i, \text{clip}\Big(\rho_{i,j}, 1{-}\varepsilon, 1{+}\varepsilon\Big) A_i\Big) - \beta D_{\text{KL}}(\pi_\theta || \pi_{\text{ref}}) \right) \right], \tag{2}$$

where D_{KL} is the KL divergence to maintain training stability, and $\rho_{i,j}$ is the ratio between the probabilities of π_θ and $\pi_{\theta_{\text{old}}}$ for outputting the current token:

$$\rho_{i,j} = \frac{\pi_\theta(y_{i,j} \mid \mathcal{P}, y_{i,<j})}{\pi_{\theta_{\text{old}}}(y_{i,j} \mid \mathcal{P}, y_{i,<j})} = \begin{cases} \dfrac{\pi_\theta\Big(y_{i,j}^{\mathcal{I}^t} | y_{i,<j}^{\mathcal{I}^t}, \mathcal{P}, \{\mathcal{I}_i^k, \mathtt{No}, \mathcal{R}_i^k\}_{k=1}^{t-1}\Big)}{\pi_{\theta_{\text{old}}}\Big(y_{i,j}^{\mathcal{I}^t} | y_{i,<j}^{\mathcal{I}^t}, \mathcal{P}, \{\mathcal{I}_i^k, \mathtt{No}, \mathcal{R}_i^k\}_{k=1}^{t-1}\Big)}, & \text{output the image in } t\text{-th round} \\[2ex] \dfrac{\pi_\theta(y_{i,j}^{\mathcal{T}^t} | y_{i,<j}^{\mathcal{T}^t}, \mathcal{P}, \{\mathcal{I}_i^k, \mathtt{No}, \mathcal{R}_i^k\}_{k=1}^{t-1}, \mathcal{I}_i^t)}{\pi_{\theta_{\text{old}}}(y_{i,j}^{\mathcal{T}^t} | y_{i,<j}^{\mathcal{T}^t}, \mathcal{P}, \{\mathcal{I}_i^k, \mathtt{No}, \mathcal{R}_i^k\}_{k=1}^{t-1}, \mathcal{I}_i^t)}, & \text{self-check the image in } t\text{-th round} \end{cases} \tag{3}$$

3.3 Towards Unified Image Generation: From T2I Generation to Image Editing

Through the above two-stage training, we introduce true CoT into visual generation, evolving the vanilla text-to-image generation into an iterative introspective process. Essentially, it is the result of the collaboration between visual comprehension and generation, which is a necessary condition for advanced image generation tasks, such as image editing. Similar to the process of introspective image generation, image editing also requires an understanding of the instructions on how to modify existing images and subsequently generate a new image. And it additionally necessitates preserving image fidelity, *i.e.*, maintaining the unedited areas in their original state.

Therefore, we only need to further teach existing models for detail preserving to easily achieve image editing capabilities. We also leverage a two-stage training for image editing: SFT and RL. **During the SFT phase**, we fine-tune the MLLM using a small number of high-quality data to learn the basic requirements of the image editing task, with the objective function denoted as: $p(y^{\mathcal{I}^{out}}) = \sum_{j=1}^{S^{\mathcal{I}}} \log P_\theta(y_j | y_{<j}, \mathcal{I}^c, \mathcal{P}^{ins})$, where $\mathcal{I}^c, \mathcal{P}^{ins}, \mathcal{I}^{out}$ are the input image, the editing instruction, and the edited image, respectively.

During the RL phase, we only provide the image condition and the editing instructions without any ground-truth images. We still leverage InternVL2.5-26B as the reward model and design two QA-based rewards: (1) Following score $\mathtt{R}^{flw} \in [0, 1]$ measures whether the model accurately follows

Table 1: Comparison with state-of-the-art models on GenEval, T2I CompBench and DPG-Bench on zero-shot text-to-image generation. The best results are in **bold fonts** with the second best underlined.

	GenEval							**T2I-CompBench**			**DPG-Bench**
Method	**Overall**↑	SingObj↑	TwoObj↑	Counting↑	Color↑	Pos. ↑	ColorAttr ↑	Color↑	Shape↑	Texture↑	Avg↑
Diffusion-based Method											
PixArt-alpha [4]	0.48	0.98	0.50	0.44	0.80	0.08	0.07	68.9	55.8	70.4	71.11
DALL-E 3 [2]	0.67	0.96	0.87	0.47	0.83	0.43	0.45	81.1	**67.5**	**80.7**	83.50
SD3 [9]	0.74	0.99	0.94	0.72	0.89	0.33	0.60	-	-	-	84.08
FLUX.1-dev [23]	0.66	0.98	0.79	0.73	0.77	0.22	0.45	-	-	-	83.79
Sana-1.5 [57]	0.81	0.99	0.93	**0.86**	0.84	0.59	0.65	-	-	-	84.70
Janus-Flow [31]	0.63	0.97	0.59	0.45	0.83	0.53	0.42	-	-	-	80.09
MLLM-based Method											
Show-o [58]	0.68	0.98	0.80	0.66	0.84	0.31	0.50	56.0	41.0	46.0	67.48
SEED-X [12]	0.49	0.96	0.57	0.29	0.82	0.14	0.15	65.7	49.2	60.3	-
Emu3 [52]	0.54	0.98	0.71	0.34	0.81	0.17	0.21	61.1	47.3	61.8	80.60
DDT-LLaMA [39]	0.66	0.99	0.64	0.56	0.87	0.39	0.48	72.8	51.4	64.2	80.90
VARGPTv1.1 [64]	0.53	0.96	0.53	0.48	0.83	0.13	0.21	-	-	-	78.59
Infinity [18]	0.73	-	0.85	-	-	0.49	0.57	-	-	-	83.46
Janus-Pro [5]	0.80	0.99	0.89	0.59	0.90	0.79	0.66	63.6	35.3	49.4	84.17
GPT-4o [34]	0.85	0.99	0.92	0.85	0.91	0.75	0.66	-	-	-	-
MLLM-based Method + CoT											
Show-o+PARM [17]	0.69	0.97	0.75	0.60	0.83	0.54	0.53	75.0	56.0	66.0	-
MINT [53]	0.73	0.98	0.82	0.66	0.79	0.55	0.56	-	-	-	-
GOT [10]	0.64	0.99	0.69	0.67	0.85	0.34	0.27	-	-	-	-
T2I-R1 [21]	-	-	-	-	-	-	-	81.3	58.5	72.4	-
Ours (w/o Aha)	0.83	0.99	0.93	0.60	0.89	0.82	0.74	81.2	56.3	73.3	85.02
Ours (with Aha)	**0.86**	**0.99**	**0.94**	0.66	**0.92**	**0.87**	**0.78**	**83.4**	59.4	75.2	**85.57**

the editing request; (2) Preserving score $\mathtt{R}^{psv} \in [0, 1]$ indicates how well the model preserves details that are not intended to be changed. And the final reward is calculated as $\mathtt{R}^{edit} = 0.5 * \mathtt{R}^{flw} + \mathtt{R}^{psv}$.

For policy gradient, we also adopt the GRPO algorithm. Given each pair of image condition and editing instruction, we sample a group of G edited images $\{\mathcal{I}_i^{out}\}_{i=1}^{G}$ from the old policy. For the i-th image response, we obtain its reward and follow Eq.(1) to obtain its advantage A_i. Finally the objective function is the same as Eq.(2). More details are given in Appendix B.

4 Experiments

We employ Janus-Pro-7B as the backbone, developing Janus-Pro-R1 and Janus-Pro-R1-Edit, excelling in text-to-image generation (§ 4.1), image editing (§ 4.2), and image semantic evaluation (§ 4.3). More details are given in Appendix C and E.

4.1 Introspective Text-to-Image Generation

Automated Metric Evaluation. We first conduct an automated metric evaluation on 3 text-to-image benchmarks: GenEval [14], T2I-CompBench [20], and DPG-Bench [19]. The comparison results against both diffusion-based and MLLM-based methods, as well as methods incorporating CoT into image generation, are presented in Table 1. We have the following observations:

(1) In most settings, our model surpasses other diffusion-based and MLLM-based baselines, achieving SOTA performance. For example, for GenEval, the overall performance of Janus-Pro-R1 even outperforms GPT-4o. This highlights that our model facilitates better vision-text alignment via unlocking the aha moment. **(2)** Compared to baselines also proposing to incorporate CoT into text-to-image generation, our method achieves superior performance, e.g., consistently outperforming concurrent work T2I-R1 on T2i-Compbench. This highlights the effectiveness of our approach in activating the true CoT for visual generation. **(3)** Compared to the backbone model Janus-Pro-7B, our method achieves performance improvements of 7.5% on Geneval, 47.0% on T2i-Compbench, and 1.7% on DPG-bench, respectively, which underscores the effectiveness of our approach. **(4)** Without activating the Aha moments and directly outputting the initial generated image, performance on the three benchmarks drops significantly, while it remains higher than that of Janus-Pro-7B, which indicates that the introspection mechanism effectively improves the image quality and the training also enhances the first-round image generation.

Qualitative Examples. In Figure 3 and Figure 7, we present qualitative examples of Janus-Pro-R1 to trigger Aha moments within its reasoning chains to generate superior images. The model could leverage its visual comprehension capabilities to accurately identify the issues in its initial-generated images, then unleash the visual generation capabilities to output a more accurate image. Even if

Table 2: Main results on PIE-Bench for image editing task.

Method	T2I Model	Structure	Background Preservation				CLIP Similarity	
		Distance ↓	PSNR ↑	LPIPS ↓	MSE ↓	SSIM ↑	Whole ↑	Edited ↑
InstructPix2Pix [3]	SD1.5 [43]	107.43	16.69	271.33	392.22	68.39	23.49	22.20
MagicBrush [61]	SD1.5	26.81	26.85	66.67	171.11	83.37	23.89	20.84
InstructDiffusion [13]	SD1.5	74.21	20.88	142.35	353.45	76.70	24.06	21.57
MGIE [11]	SD1.5	67.41	21.20	142.25	295.11	77.52	24.28	21.79
Seed-X-Edit [12]	SD-XL [43]	61.69	18.80	173.63	209.05	74.93	25.51	22.20
EditAR [32]	LlamaGen [46]	39.43	21.32	117.15	130.27	75.13	24.87	21.87
Janus-Pro-Edit	Janus-Pro [5]	49.44	20.50	131.76	185.04	73.29	24.16	21.60
Janus-Pro-R1-Edit (Ours)	Janus-Pro-R1	35.87	22.81	114.96	123.30	76.80	24.78	22.31

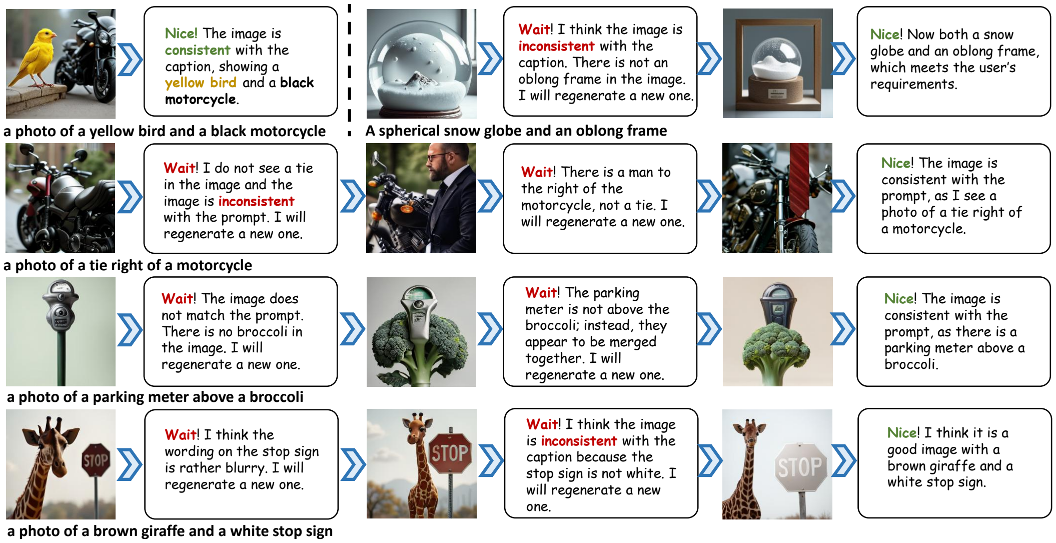

Nice! The image is consistent with the caption, showing a yellow bird and a black motorcycle.

a photo of a yellow bird and a black motorcycle

Wait! I think the image is inconsistent with the caption. There is not an oblong frame in the image. I will regenerate a new one.

Nice! Now both a snow globe and an oblong frame, which meets the user's requirements.

A spherical snow globe and an oblong frame

Wait! I do not see a tie in the image and the image is inconsistent with the prompt. I will regenerate a new one.

Wait! There is a man to the right of the motorcycle, not a tie. I will regenerate a new one.

Nice! The image is consistent with the prompt, as I see a photo of a tie right of a motorcycle.

a photo of a tie right of a motorcycle

Wait! The image does not match the prompt. There is no broccoli in the image. I will regenerate a new one.

Wait! The parking meter is not above the broccoli; instead, they appear to be merged together. I will regenerate a new one.

Nice! The image is consistent with the prompt, as there is a parking meter above a broccoli.

a photo of a parking meter above a broccoli

Wait! I think the wording on the stop sign is rather blurry. I will regenerate a new one.

Wait! I think the image is inconsistent with the caption because the stop sign is not white. I will regenerate a new one.

Nice! I think it is a good image with a brown giraffe and a white stop sign.

a photo of a brown giraffe and a white stop sign

Figure 3: Qualitative examples of introspective text-to-image generation that triggers Aha moments.

the newly generated image still fails to meet the requirements, the model can trigger a second Aha moment, re-evaluating the issues and repeating the visual generation to produce a fully compliant image.

4.2 Image Editing

Automated Metric Evaluation. We use PIE-Bench [22] as the evaluation benchmark for image editing. We compare with instruction-based large-scale training methods, with structure distance and background preservation metrics reflecting fidelity preservation, while CLIP similarity is used for editability evaluation. As shown in Table 2, most existing methods fail to achieve a good balance between fidelity and editability. While EditAR, which employs the AR framework, demonstrate a relatively better trade-off. Compared to these baselines, Janus-Pro-R1-Edit achieves better overall performance and maintains a good balance between fidelity and editability. Especially compared with EditAR, it excels in most metrics with superior performance.

Qualitative Examples. We also conduct a qualitative comparison with both open-source [61, 62] and closed-source [34, 49] leading works on multi-turn editing in Figure 4. Our model supports a wide range of editing operations, with the output images consistently resembling the source images while remaining coherent with the instructions. This stable trade-off between fidelity and editability is rarely achieved in open-source models, and in some cases, our results even outperform closed-source models such as Gemini-2.0 [49].

4.3 Janus-Pro-R1 as a Stronger Image Semantic Evaluator

After two-stage training, we find that Janus-Pro-R1 also emerges as an excellent image semantic evaluator. Specifically, it can: (1) Assess whether a given image-text pair is consistent, serving as an evaluation function for text-to-image benchmarking; (2) act as a reward model for text-to-image RL in place of visual comprehension models, enhancing the performance of other text-to-image models.

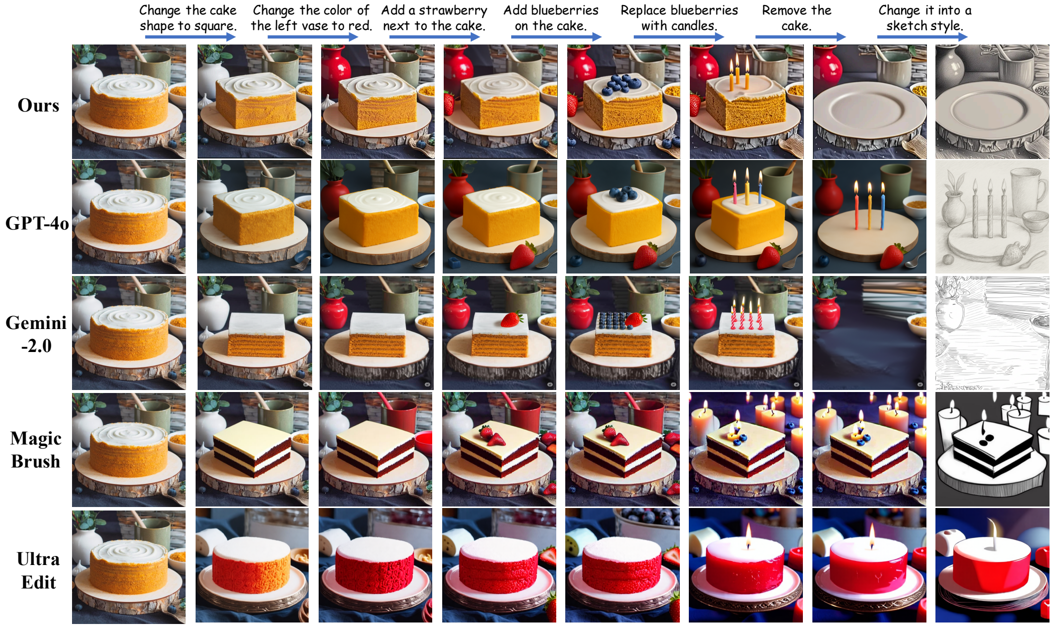
Change the cake shape to square.
Change the color of the left vase to red.
Add a strawberry next to the cake.
Add blueberries on the cake.
Replace blueberries with candles.
Remove the cake.
Change it into a sketch style.
Ours
GPT-4o
Gemini -2.0
Magic Brush
Ultra Edit

Figure 4: Our model achieve a stable trade-off between fidelity and editability in multi-turn editing.

Evaluation Metric for Text-to-Image Benchmarking. We first instruct a text-to-image model Janus-Pro-1B to generate over 2, 000 images for GenEval, and use the original object-focused framework within the benchmark as the standard for text-to-image alignment evaluation. Then we leverage Janus-Pro-7B, Janus-Pro-SFT (7B, only undergoing the first-stage SFT training without RL), and InternVL2.5-8B, and Janus-Pro-R1 (7B) as the evaluation functions, comparing their results with those of the standard evaluation framework. As shown in Table 3, Janus-Pro-R1 achieves an 81.1% consistency ratio with the standard framework's assessment. In contrast, Janus-Pro-7B, Janus-Pro-SFT-7B, and InternVL2.5-8B consistently exhibit lower consistency ratios compared to Janus-Pro-R1.

Table 3: The consistency ratio with the standard assessment on GenEval, and the reason reliability score evaluated by GPT-4o, when utilizing different models for text-image alignment evaluation.

Method	Consistency Ratio on GenEval (%)	Reason Reliability Score by GPT-4o
Janus-Pro-7B	72.3	76.9
Janus-Pro-SFT (7B)	72.7	78.8
InternVL2.5 (8B)	79.0	**92.2**
Janus-Pro-R1 (7B)	**81.1**	91.1

Furthermore, we collect several hundred pairs of semantically mismatched text-image pairs. We require the above four models to determine whether the semantics of the image and text are matched and to provide relevant reasons. We then use GPT-4o as the evaluation model to score the reasons provided by the four models from 0 (unreasonable) to 1 (reasonable). As shown in Table 3, Janus-Pro-R1 outperforms both Janus-Pro-7B and Janus-Pro-SFT in providing reasons that are deemed more reliable by GPT-4o. It even approaches the performance of the comprehension-only MLLM, *i.e.*, InternVL2.5-8B. These results indicate that **(1)** compared to the backbone model and even a comprehension-only MLLM, Janus-Pro-R1 more closely aligns with the standard metrics within GenEval, achieving greater evaluation precision; and **(2)** the visual comprehension capability of our model is significantly enhanced after reinforcement learning. In contrast, SFT only endows the MLLM with the basic capability for combining visual comprehension and generation, resulting in only incremental improvements to its inherent multimodal understanding ability.

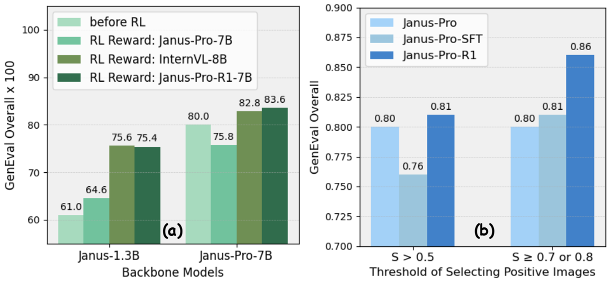

Figure 5: (a) RL Performance with different reward models. (b) Performance with different selecting thresholds in SFT.

Table 4: Zero-shot text-to-image performance on GenEval of different models for in-depth analysis

	Method	Overall↑	SingObj↑	TwoObj↑	Counting↑	Color↑	Pos. ↑	ColorAttr ↑
1	Janus-Pro *(7B)*	0.80	0.99	0.89	0.59	0.90	0.79	0.66
2	Janus-Pro-SFT *(7B, w/o aha)*	0.81	0.98	0.88	0.59	0.89	0.80	0.70
3	Janus-Pro-SFT *(7B, with aha)*	0.81	0.99	0.87	0.57	0.90	0.81	0.72
4	Janus-Pro-R1 *(7B, w/o aha)*	0.83	0.99	0.93	0.60	0.89	0.82	0.74
5	Janus-Pro-R1 *(7B, with aha)*	**0.86**	**0.99**	**0.94**	**0.66**	**0.92**	**0.87**	**0.78**
6	Janus-Pro-SFT1 *(7B, Task-I, w/o aha)*	0.79	0.98	0.88	0.56	0.89	0.76	0.65
7	Janus-Pro-SFT2 *(7B, Task-II+Task-III, with aha)*	0.76	0.98	0.86	0.55	0.85	0.73	0.61
8	Janus-Pro *(1B)*	0.73	0.98	0.82	0.51	0.89	0.65	0.56
9	Janus-Pro-R1 *(1B, w/o aha)*	0.70	0.95	0.78	0.53	0.82	0.60	0.52
10	Janus-Pro-R1 *(1B, with aha)*	0.71	0.98	0.80	0.51	0.84	0.59	0.55

Reward Model for Text-to-Image RL. With Janus-Pro-7B and Janus-1.3B [55] as backbone models, we employ Janus-Pro-7B, InternVL2.5-8B [6] and Janus-Pro-R1 as reward models to provide text-image consistency scores as the incentives for text-to-image RL. As shown in Figure 5(a), using Janus-Pro-R1 as the reward model significantly enhances the overall performance of both backbone models on GenEval following reinforcement learning, outperforming the results with InternVL2.5-8B as the reward model. The results highlight the superior visual comprehension capability of our model, which can more accurately assess the text-image semantic consistency.

4.4 In-Depth Analysis

Introspective Text-to-Image Enables Better Image Editing. To further demonstrate that introspective text-to-image generation with the collaboration between visual comprehension and generation, could enable better image editing, we directly apply the same training paradigm described in § 3.3 to Janus-Pro-7B (we name it as Janus-Pro-Edit). As shown in Table 2, Janus-Pro-R1-Edit consistently outperformed Janus-Pro-Edit on Pie-bench in both instruction following and unedited area preservation, which further validates the effectiveness of our approach.

Effect of Model Scale to Unlock Aha Moments. We further employ Janus-Pro-1B as the backbone to explore whether a smaller model could also achieve a breakthrough in visual generation going through the same training paradigm. As shown in Table 4 **Rows 8-10**, in contrast to the significant performance improvement observed in Janus-Pro-R1-7B, Janus-Pro-R1-1B does not achieve superior image generation performance compared to the backbone. And the attempt to activate the Aha moments in this 1B model even compromises its initial image generation capabilities. This suggests that the CoT with deep thinking for visual generation requires a larger parameter size to be effectively handled, which is also an illustration of the scaling law.

Effect of Data Quality in SFT. During SFT, when selecting positive images for subtask training, we establish a higher threshold larger than 0.5 of the semantic consistent score ($\mathcal{S} \geq 0.7$ for comprehension tasks and $\mathcal{S} \geq 0.8$ for generation tasks). Though a higher threshold reduces the quantity of available training data, we find that it is crucial for improving performance. In contrast, we also set the threshold as $\mathcal{S} > 0.5$ for selecting positive images in all three subtasks. As shown in Figure 5(b), the decrease in data quality leads to degraded T2I performance of both post-SFT and post-RL models. This highlights that the quality of SFT data is more important than its quantity.

Synergy of Sub-Tasks in SFT. We further demonstrate that in SFT, the text-to-image generation capability from Task-I and the regeneration abilities derived from Task-II and Task-III are synergistic. We train two ablation models: Janus-Pro-SFT-1, which undergoes only text-to-image SFT with task-I, and Janus-Pro-SFT-2, which undergoes the mixed SFT of task-II and task-III. As shown in Table 4 **Rows 6-7**, in GenEval, the initial image generation quality of Janus-Pro-SFT is superior to that of Janus-Pro-SFT-1, and the final image generation quality after self-correction is superior to that of Janus-Pro-SFT-2. This indicates that the capabilities of simple text-to-image generation and multi-round image regeneration mutually enhance each other in a synergistic manner.

SFT Memorizes, RL Generalizes. We compare the text-to-image performance change after the SFT phase (*i.e.,* Janus-Pro-SFT) and the RL phase (*i.e.,* Janus-Pro-R1). First, as shown in Table 4 **Rows 1-5**, After SFT, the performance improvement compared to the backbone model Janus-Pro-7B is minimal, with image regeneration not significantly improving the quality of the first generated image. This is because SFT tends to enable the model to imitate and memorize some sub-skills to develop the visual generation CoT, lacking the ability of generalization. In contrast, RL enhances

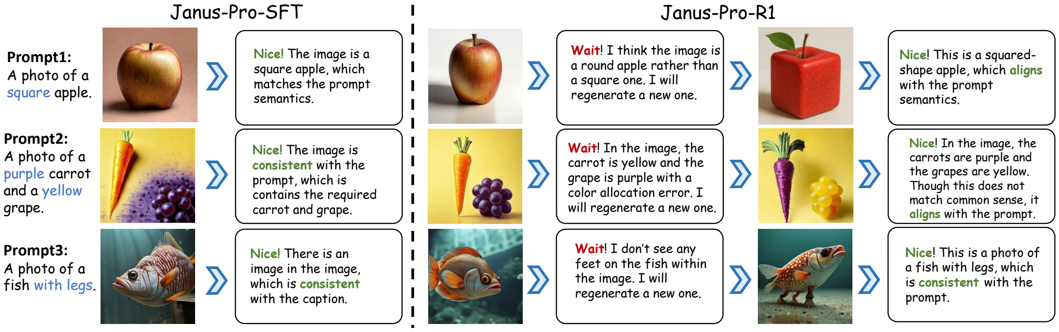
Janus-Pro-SFT
Janus-Pro-R1
Prompt1:
A photo of a square apple.
Nice! The image is a square apple, which matches the prompt semantics.
Wait! I think the image is a round apple rather than a square one. I will regenerate a new one.
Nice! This is a squared-shape apple, which aligns with the prompt semantics.
Prompt2:
A photo of a purple carrot and a yellow grape.
Nice! The image is consistent with the prompt, which is contains the required carrot and grape.
Wait! In the image, the carrot is yellow and the grape is purple with a color allocation error. I will regenerate a new one.
Nice! In the image, the carrots are purple and the grapes are yellow. Though this does not match common sense, it aligns with the prompt.
Prompt3:
A photo of a fish with legs.
Nice! There is an image in the image, which is consistent with the caption.
Wait! I don't see any feet on the fish within the image. I will regenerate a new one.
Nice! This is a photo of a fish with legs, which is consistent with the prompt.

Figure 6: Performance of Janus-Pro-SFT and Janus-Pro-R1 for counterfactual generation.

generalization, significantly improving both the quality of the generated images and ensuring that the introspection process is genuinely effective. Of course, SFT is still essential, as it serves the role as cold-start and provides the foundation for the MLLM to explore reliable visual generation CoTs.

In Figure 6, we further present cases of counterfactual generation to highlight the differences between Janus-Pro-SFT and Janus-Pro-R1. When given counterfactual prompts such as "a square apple", both models initially generate images that do not align with the prompt due to ingrained common-sense. However, Janus-Pro-SFT deems the initial image reasonable as the final output. In contrast, Janus-Pro-R1 identifies the semantic mismatches in the initial image and regenerates a new one that meets the requirements. This demonstrates that RL could generalize the original imitative behavior after SFT to genuine reasoning, thereby better avoiding the generation of hallucinations.

RL Paves the Way for Genuine Unified Visual Comprehension and Generation. The essence of unification for comprehension and generation should be reflected in the synergistic enhancement between the two capabilities. So what kind of training paradigm can promote such unification? From Tables 4 (**Rows 1-5**) and 3, we observe that although we can endow models with the foundational ability to collaborate on visual comprehension and generation through SFT, the model appears to merely mechanically mimic and combine these two skills. The combination does not bring about any substantial improvement to either capability. Specifically, the performance of Janus-Pro-SFT-7B in both the visual comprehension task of image-text semantic consistency judgment and the text-to-image generation task shows very incremental improvement compared to Janus-Pro-7B. However, through RL, we encourage the model to spontaneously integrate the two capabilities to explore reasoning pathways, and merely provide incentives as appropriate guidance. We find that the model learns how to better coordinate these two capabilities, resulting in stronger text-to-image generation and image semantic understanding abilities.

Therefore, we argue that ***RL holds the potential to unlock genuine unified visual comprehension and generation***. However, the current experiments are insufficient to conclusively validate this assertion. Owing to limited computational resources, our conclusion is based solely on simple image generation tasks and text-image semantic alignment evaluation tasks. Nevertheless, the experiments do provide some preliminary evidence for this conclusion. Given adequate computational resources, we think that large-scale RL could feasibly be employed to achieve a synergistic enhancement of visual comprehension and generation for genuine unification, empowering MLLMs to demonstrate powerful image understanding and generation capabilities comparable to GPT-4o.

5 Conclusion

In this paper, we enable MLLMs to form a genuine CoT via deep thinking, advancing text-to-image generation into an iterative introspective process, thereby unlocking the Aha moments in visual generation. We introduce a two-stage training paradigm: SFT teaches the MLLM with the foundational ability to generate visual generation CoT with task decomposition, while RL effectively balances the exploration–exploitation trade-off to unlock its full potential. On this basis, we further endow the MLLM with unified visual generation capabilities, such as image editing. Extensive experiments demonstrate that our model achieves superior performance in both text-to-image generation and image editing tasks, also serving as an excellent image semantic evaluator.

Acknowledgements

This work was supported by the Key R&D Projects in Zhejiang Province (No. 2024C01106, 2025C01030), the NSFC (62272411), the Zhejiang NSF (LRG25F020001) and Ant Group, My Bank.

References

[1] Jinze Bai, Shuai Bai, Yunfei Chu, Zeyu Cui, Kai Dang, Xiaodong Deng, Yang Fan, Wenbin Ge, Yu Han, Fei Huang, Binyuan Hui, Luo Ji, Mei Li, Junyang Lin, Runji Lin, Dayiheng Liu, Gao Liu, Chengqiang Lu, Keming Lu, Jianxin Ma, Rui Men, Xingzhang Ren, Xuancheng Ren, Chuanqi Tan, Sinan Tan, Jianhong Tu, Peng Wang, Shijie Wang, Wei Wang, Shengguang Wu, Benfeng Xu, Jin Xu, An Yang, Hao Yang, Jian Yang, Shusheng Yang, Yang Yao, Bowen Yu, Hongyi Yuan, Zheng Yuan, Jianwei Zhang, Xingxuan Zhang, Yichang Zhang, Zhenru Zhang, Chang Zhou, Jingren Zhou, Xiaohuan Zhou, and Tianhang Zhu. Qwen technical report. *arXiv preprint arXiv:2309.16609*, 2023.

[2] James Betker, Gabriel Goh, Li Jing, Tim Brooks, Jianfeng Wang, Linjie Li, Long Ouyang, Juntang Zhuang, Joyce Lee, Yufei Guo, et al. Improving image generation with better captions. *Computer Science. https://cdn. openai. com/papers/dall-e-3. pdf*, 2(3):8, 2023.

[3] Tim Brooks, Aleksander Holynski, and Alexei A Efros. Instructpix2pix: Learning to follow image editing instructions. In *Proceedings of the IEEE/CVF conference on computer vision and pattern recognition*, pages 18392–18402, 2023.

[4] Junsong Chen, Jincheng Yu, Chongjian Ge, Lewei Yao, Enze Xie, Yue Wu, Zhongdao Wang, James Kwok, Ping Luo, Huchuan Lu, and Zhenguo Li. Pixart-α: Fast training of diffusion transformer for photorealistic text-to-image synthesis, 2023.

[5] Xiaokang Chen, Zhiyu Wu, Xingchao Liu, Zizheng Pan, Wen Liu, Zhenda Xie, Xingkai Yu, and Chong Ruan. Janus-pro: Unified multimodal understanding and generation with data and model scaling. *arXiv preprint arXiv:2501.17811*, 2025.

[6] Zhe Chen, Jiannan Wu, Wenhai Wang, Weijie Su, Guo Chen, Sen Xing, Muyan Zhong, Qinglong Zhang, Xizhou Zhu, Lewei Lu, et al. Internvl: Scaling up vision foundation models and aligning for generic visual-linguistic tasks. In *Proceedings of the IEEE/CVF Conference on Computer Vision and Pattern Recognition*, pages 24185–24198, 2024.

[7] Jaemin Cho, Yushi Hu, Jason Baldridge, Roopal Garg, Peter Anderson, Ranjay Krishna, Mohit Bansal, Jordi Pont-Tuset, and Su Wang. Davidsonian scene graph: Improving reliability in fine-grained evaluation for text-to-image generation. In *ICLR*, 2024.

[8] Wei Chow, Juncheng Li, Qifan Yu, Kaihang Pan, Hao Fei, Zhiqi Ge, Shuai Yang, Siliang Tang, Hanwang Zhang, and Qianru Sun. Unified generative and discriminative training for multi-modal large language models. *arXiv preprint arXiv:2411.00304*, 2024.

[9] Patrick Esser, Sumith Kulal, Andreas Blattmann, Rahim Entezari, Jonas Müller, Harry Saini, Yam Levi, Dominik Lorenz, Axel Sauer, Frederic Boesel, et al. Scaling rectified flow transformers for high-resolution image synthesis. In *Forty-first international conference on machine learning*, 2024.

[10] Rongyao Fang, Chengqi Duan, Kun Wang, Linjiang Huang, Hao Li, Shilin Yan, Hao Tian, Xingyu Zeng, Rui Zhao, Jifeng Dai, et al. Got: Unleashing reasoning capability of multimodal large language model for visual generation and editing. *arXiv preprint arXiv:2503.10639*, 2025.

[11] Tsu-Jui Fu, Wenze Hu, Xianzhi Du, William Yang Wang, Yinfei Yang, and Zhe Gan. Guiding instruction-based image editing via multimodal large language models. *arXiv preprint arXiv:2309.17102*, 2023.

[12] Yuying Ge, Sijie Zhao, Jinguo Zhu, Yixiao Ge, Kun Yi, Lin Song, Chen Li, Xiaohan Ding, and Ying Shan. Seed-x: Multimodal models with unified multi-granularity comprehension and generation. *arXiv preprint arXiv:2404.14396*, 2024.

[13] Zigang Geng, Binxin Yang, Tiankai Hang, Chen Li, Shuyang Gu, Ting Zhang, Jianmin Bao, Zheng Zhang, Houqiang Li, Han Hu, et al. Instructdiffusion: A generalist modeling interface for vision tasks. In *Proceedings of the IEEE/CVF Conference on computer vision and pattern recognition*, pages 12709–12720, 2024.

[14] Dhruba Ghosh, Hannaneh Hajishirzi, and Ludwig Schmidt. Geneval: An object-focused framework for evaluating text-to-image alignment. *Advances in Neural Information Processing Systems*, 36:52132–52152, 2023.

[15] Xin Gu, Ming Li, Libo Zhang, Fan Chen, Longyin Wen, Tiejian Luo, and Sijie Zhu. Multi-reward as condition for instruction-based image editing. *arXiv preprint arXiv:2411.04713*, 2024.

[16] Daya Guo, Dejian Yang, Haowei Zhang, Junxiao Song, Ruoyu Zhang, Runxin Xu, Qihao Zhu, Shirong Ma, Peiyi Wang, Xiao Bi, et al. Deepseek-r1: Incentivizing reasoning capability in llms via reinforcement learning. *arXiv preprint arXiv:2501.12948*, 2025.

[17] Ziyu Guo, Renrui Zhang, Chengzhuo Tong, Zhizheng Zhao, Peng Gao, Hongsheng Li, and Pheng-Ann Heng. Can we generate images with cot? let's verify and reinforce image generation step by step, 2025.

[18] Jian Han, Jinlai Liu, Yi Jiang, Bin Yan, Yuqi Zhang, Zehuan Yuan, Bingyue Peng, and Xiaobing Liu. Infinity: Scaling bitwise autoregressive modeling for high-resolution image synthesis. *arXiv preprint arXiv:2412.04431*, 2024.

[19] Xiwei Hu, Rui Wang, Yixiao Fang, Bin Fu, Pei Cheng, and Gang Yu. Ella: Equip diffusion models with llm for enhanced semantic alignment. *arXiv preprint arXiv:2403.05135*, 2024.

[20] Kaiyi Huang, Kaiyue Sun, Enze Xie, Zhenguo Li, and Xihui Liu. T2i-compbench: A comprehensive benchmark for open-world compositional text-to-image generation. *Advances in Neural Information Processing Systems*, 36:78723–78747, 2023.

[21] Dongzhi Jiang, Ziyu Guo, Renrui Zhang, Zhuofan Zong, Hao Li, Le Zhuo, Shilin Yan, Pheng-Ann Heng, and Hongsheng Li. T2i-r1: Reinforcing image generation with collaborative semantic-level and token-level cot. *arXiv preprint arXiv:2505.00703*, 2025.

[22] Xuan Ju, Ailing Zeng, Yuxuan Bian, Shaoteng Liu, and Qiang Xu. Pnp inversion: Boosting diffusion-based editing with 3 lines of code. *International Conference on Learning Representations (ICLR)*, 2024.

[23] Black Forest Labs. Flux. `https://github.com/black-forest-labs/flux`, 2024.

[24] Bo Li, Yuanhan Zhang, Dong Guo, Renrui Zhang, Feng Li, Hao Zhang, Kaichen Zhang, Peiyuan Zhang, Yanwei Li, Ziwei Liu, et al. Llava-onevision: Easy visual task transfer. *arXiv preprint arXiv:2408.03326*, 2024.

[25] Juncheng Li, Kaihang Pan, Zhiqi Ge, Minghe Gao, Wei Ji, Wenqiao Zhang, Tat-Seng Chua, Siliang Tang, Hanwang Zhang, and Yueting Zhuang. Fine-tuning multimodal llms to follow zero-shot demonstrative instructions. *arXiv preprint arXiv:2308.04152*, 2023.

[26] Junnan Li, Dongxu Li, Caiming Xiong, and Steven Hoi. Blip: Bootstrapping language-image pre-training for unified vision-language understanding and generation. In *International conference on machine learning*, pages 12888–12900. PMLR, 2022.

[27] Wang Lin, Liyu Jia, Wentao Hu, Kaihang Pan, Zhongqi Yue, Wei Zhao, Jingyuan Chen, Fei Wu, and Hanwang Zhang. Reasoning physical video generation with diffusion timestep tokens via reinforcement learning. *arXiv preprint arXiv:2504.15932*, 2025.

[28] Hao Liu, Wilson Yan, Matei Zaharia, and Pieter Abbeel. World model on million-length video and language with blockwise ringattention. *arXiv preprint arXiv:2402.08268*, 2024.

[29] Haotian Liu, Chunyuan Li, Yuheng Li, and Yong Jae Lee. Improved baselines with visual instruction tuning. In *Proceedings of the IEEE/CVF Conference on Computer Vision and Pattern Recognition*, pages 26296–26306, 2024.

[30] Haotian Liu, Chunyuan Li, Qingyang Wu, and Yong Jae Lee. Visual instruction tuning. *Advances in neural information processing systems*, 36:34892–34916, 2023.

[31] Yiyang Ma, Xingchao Liu, Xiaokang Chen, Wen Liu, Chengyue Wu, Zhiyu Wu, Zizheng Pan, Zhenda Xie, Haowei Zhang, Xingkai yu, Liang Zhao, Yisong Wang, Jiaying Liu, and Chong Ruan. Janusflow: Harmonizing autoregression and rectified flow for unified multimodal understanding and generation, 2024.

[32] Jiteng Mu, Nuno Vasconcelos, and Xiaolong Wang. Editar: Unified conditional generation with autoregressive models. *arXiv preprint arXiv:2501.04699*, 2025.

[33] OpenAI. Chatgpt. `https://chat.openai.com`, 2023.

[34] OpenAI. Introducing 4o image generation. `https://openai.com/index/introducing-4o-image-generation/`, 2024.

[35] Kaihang Pan, Wendong Bu, Yuruo Wu, Yang Wu, Kai Shen, Yunfei Li, Hang Zhao, Juncheng Li, Siliang Tang, and Yueting Zhuang. Focusdiff: Advancing fine-grained text-image alignment for autoregressive visual generation through rl. *arXiv preprint arXiv:2506.05501*, 2025.

[36] Kaihang Pan, Zhaoyu Fan, Juncheng Li, Qifan Yu, Hao Fei, Siliang Tang, Richang Hong, Hanwang Zhang, and Qianru Sun. Towards unified multimodal editing with enhanced knowledge collaboration. *Advances in Neural Information Processing Systems*, 37:110290–110314, 2024.

[37] Kaihang Pan, Juncheng Li, Hongye Song, Jun Lin, Xiaozhong Liu, and Siliang Tang. Self-supervised meta-prompt learning with meta-gradient regularization for few-shot generalization. *arXiv preprint arXiv:2303.12314*, 2023.

[38] Kaihang Pan, Juncheng Li, Wenjie Wang, Hao Fei, Hongye Song, Wei Ji, Jun Lin, Xiaozhong Liu, Tat-Seng Chua, and Siliang Tang. I3: I ntent-i ntrospective retrieval conditioned on i nstructions. In *Proceedings of the 47th International ACM SIGIR Conference on Research and Development in Information Retrieval*, pages 1839–1849, 2024.

[39] Kaihang Pan, Wang Lin, Zhongqi Yue, Tenglong Ao, Liyu Jia, Wei Zhao, Juncheng Li, Siliang Tang, and Hanwang Zhang. Generative multimodal pretraining with discrete diffusion timestep tokens. In *Proceedings of the Computer Vision and Pattern Recognition Conference*, pages 26136–26146, 2025.

[40] Kaihang Pan, Siliang Tang, Juncheng Li, Zhaoyu Fan, Wei Chow, Shuicheng Yan, Tat-Seng Chua, Yueting Zhuang, and Hanwang Zhang. Auto-encoding morph-tokens for multimodal llm. *arXiv preprint arXiv:2405.01926*, 2024.

[41] Mohit Prabhushankar and Ghassan AlRegib. Introspective learning: A two-stage approach for inference in neural networks. *Advances in Neural Information Processing Systems*, 35:12126–12140, 2022.

[42] Haiyi Qiu, Minghe Gao, Long Qian, Kaihang Pan, Qifan Yu, Juncheng Li, Wenjie Wang, Siliang Tang, Yueting Zhuang, and Tat-Seng Chua. Step: Enhancing video-llms' compositional reasoning by spatio-temporal graph-guided self-training. *arXiv preprint arXiv:2412.00161*, 2024.

[43] Robin Rombach, Andreas Blattmann, Dominik Lorenz, Patrick Esser, and Björn Ommer. High-resolution image synthesis with latent diffusion models. In *Proceedings of the IEEE/CVF conference on computer vision and pattern recognition*, pages 10684–10695, 2022.

[44] John Schulman, Filip Wolski, Prafulla Dhariwal, Alec Radford, and Oleg Klimov. Proximal policy optimization algorithms. *arXiv preprint arXiv:1707.06347*, 2017.

[45] Zhihong Shao, Peiyi Wang, Qihao Zhu, Runxin Xu, Junxiao Song, Xiao Bi, Haowei Zhang, Mingchuan Zhang, YK Li, Y Wu, et al. Deepseekmath: Pushing the limits of mathematical reasoning in open language models. *arXiv preprint arXiv:2402.03300*, 2024.

[46] Peize Sun, Yi Jiang, Shoufa Chen, Shilong Zhang, Bingyue Peng, Ping Luo, and Zehuan Yuan. Autoregressive model beats diffusion: Llama for scalable image generation. *arXiv preprint arXiv:2406.06525*, 2024.

[47] Quan Sun, Yufeng Cui, Xiaosong Zhang, Fan Zhang, Qiying Yu, Yueze Wang, Yongming Rao, Jingjing Liu, Tiejun Huang, and Xinlong Wang. Generative multimodal models are in-context learners. In *Proceedings of the IEEE/CVF Conference on Computer Vision and Pattern Recognition*, pages 14398–14409, 2024.

[48] Lukasz Szpruch, Tanut Treetanthiploet, and Yufei Zhang. Exploration-exploitation trade-off for continuous-time episodic reinforcement learning with linear-convex models. *arXiv preprint arXiv:2112.10264*, 2021.

[49] Gemini Team, Rohan Anil, Sebastian Borgeaud, Jean-Baptiste Alayrac, Jiahui Yu, Radu Soricut, Johan Schalkwyk, Andrew M Dai, Anja Hauth, Katie Millican, et al. Gemini: a family of highly capable multimodal models. *arXiv preprint arXiv:2312.11805*, 2023.

[50] Shengbang Tong, David Fan, Jiachen Zhu, Yunyang Xiong, Xinlei Chen, Koustuv Sinha, Michael Rabbat, Yann LeCun, Saining Xie, and Zhuang Liu. Metamorph: Multimodal understanding and generation via instruction tuning. *arXiv preprint arXiv:2412.14164*, 2024.

[51] Bohan Wang, Zhongqi Yue, Fengda Zhang, Shuo Chen, Li'an Bi, Junzhe Zhang, Xue Song, Kennard Yanting Chan, Jiachun Pan, Weijia Wu, et al. Discrete visual tokens of autoregression, by diffusion, and for reasoning. *arXiv preprint arXiv:2505.07538*, 2025.

[52] Xinlong Wang, Xiaosong Zhang, Zhengxiong Luo, Quan Sun, Yufeng Cui, Jinsheng Wang, Fan Zhang, Yueze Wang, Zhen Li, Qiying Yu, et al. Emu3: Next-token prediction is all you need. *arXiv preprint arXiv:2409.18869*, 2024.

[53] Yi Wang, Mushui Liu, Wanggui He, Longxiang Zhang, Ziwei Huang, Guanghao Zhang, Fangxun Shu, Zhong Tao, Dong She, Zhelun Yu, et al. Mint: Multi-modal chain of thought in unified generative models for enhanced image generation. *arXiv preprint arXiv:2503.01298*, 2025.

[54] Jason Wei, Xuezhi Wang, Dale Schuurmans, Maarten Bosma, Fei Xia, Ed Chi, Quoc V Le, Denny Zhou, et al. Chain-of-thought prompting elicits reasoning in large language models. *Advances in neural information processing systems*, 35:24824–24837, 2022.

[55] Chengyue Wu, Xiaokang Chen, Zhiyu Wu, Yiyang Ma, Xingchao Liu, Zizheng Pan, Wen Liu, Zhenda Xie, Xingkai Yu, Chong Ruan, et al. Janus: Decoupling visual encoding for unified multimodal understanding and generation. *arXiv preprint arXiv:2410.13848*, 2024.

[56] Shitao Xiao, Yueze Wang, Junjie Zhou, Huaying Yuan, Xingrun Xing, Ruiran Yan, Chaofan Li, Shuting Wang, Tiejun Huang, and Zheng Liu. Omnigen: Unified image generation. *arXiv preprint arXiv:2409.11340*, 2024.

[57] Enze Xie, Junsong Chen, Yuyang Zhao, Jincheng Yu, Ligeng Zhu, Chengyue Wu, Yujun Lin, Zhekai Zhang, Muyang Li, Junyu Chen, et al. Sana 1.5: Efficient scaling of training-time and inference-time compute in linear diffusion transformer. *arXiv preprint arXiv:2501.18427*, 2025.

[58] Jinheng Xie, Weijia Mao, Zechen Bai, David Junhao Zhang, Weihao Wang, Kevin Qinghong Lin, Yuchao Gu, Zhijie Chen, Zhenheng Yang, and Mike Zheng Shou. Show-o: One single transformer to unify multimodal understanding and generation. *arXiv preprint arXiv:2408.12528*, 2024.

[59] Qifan Yu, Wei Chow, Zhongqi Yue, Kaihang Pan, Yang Wu, Xiaoyang Wan, Juncheng Li, Siliang Tang, Hanwang Zhang, and Yueting Zhuang. Anyedit: Mastering unified high-quality image editing for any idea. *arXiv preprint arXiv:2411.15738*, 2024.

[60] Xiaohua Zhai, Basil Mustafa, Alexander Kolesnikov, and Lucas Beyer. Sigmoid loss for language image pre-training. In *Proceedings of the IEEE/CVF international conference on computer vision*, pages 11975–11986, 2023.

[61] Kai Zhang, Lingbo Mo, Wenhu Chen, Huan Sun, and Yu Su. Magicbrush: A manually annotated dataset for instruction-guided image editing. *Advances in Neural Information Processing Systems*, 36:31428–31449, 2023.

[62] Haozhe Zhao, Xiaojian Shawn Ma, Liang Chen, Shuzheng Si, Rujie Wu, Kaikai An, Peiyu Yu, Minjia Zhang, Qing Li, and Baobao Chang. Ultraedit: Instruction-based fine-grained image editing at scale. *Advances in Neural Information Processing Systems*, 37:3058–3093, 2024.

[63] Chunting Zhou, Lili Yu, Arun Babu, Kushal Tirumala, Michihiro Yasunaga, Leonid Shamis, Jacob Kahn, Xuezhe Ma, Luke Zettlemoyer, and Omer Levy. Transfusion: Predict the next token and diffuse images with one multi-modal model. *arXiv preprint arXiv:2408.11039*, 2024.

[64] Xianwei Zhuang, Yuxin Xie, Yufan Deng, Dongchao Yang, Liming Liang, Jinghan Ru, Yuguo Yin, and Yuexian Zou. Vargpt-v1. 1: Improve visual autoregressive large unified model via iterative instruction tuning and reinforcement learning. *arXiv preprint arXiv:2504.02949*, 2025.

NeurIPS Paper Checklist

1. **Claims**

   Question: Do the main claims made in the abstract and introduction accurately reflect the paper's contributions and scope?

   Answer: [Yes]

   Justification: The Abstract and Section 1 (Introduction) of our paper clearly reflect the contributions and scope, including the proposed method, addressed problems.

   Guidelines:

   - The answer NA means that the abstract and introduction do not include the claims made in the paper.
   - The abstract and/or introduction should clearly state the claims made, including the contributions made in the paper and important assumptions and limitations. A No or NA answer to this question will not be perceived well by the reviewers.
   - The claims made should match theoretical and experimental results, and reflect how much the results can be expected to generalize to other settings.
   - It is fine to include aspirational goals as motivation as long as it is clear that these goals are not attained by the paper.

2. **Limitations**

   Question: Does the paper discuss the limitations of the work performed by the authors?

   Answer: [Yes]

   Justification: We explicitly discuss the limitations of our work in the appendix within the Supplementary Material.

   Guidelines:

   - The answer NA means that the paper has no limitation while the answer No means that the paper has limitations, but those are not discussed in the paper.
   - The authors are encouraged to create a separate "Limitations" section in their paper.
   - The paper should point out any strong assumptions and how robust the results are to violations of these assumptions (e.g., independence assumptions, noiseless settings, model well-specification, asymptotic approximations only holding locally). The authors should reflect on how these assumptions might be violated in practice and what the implications would be.
   - The authors should reflect on the scope of the claims made, e.g., if the approach was only tested on a few datasets or with a few runs. In general, empirical results often depend on implicit assumptions, which should be articulated.
   - The authors should reflect on the factors that influence the performance of the approach. For example, a facial recognition algorithm may perform poorly when image resolution is low or images are taken in low lighting. Or a speech-to-text system might not be used reliably to provide closed captions for online lectures because it fails to handle technical jargon.
   - The authors should discuss the computational efficiency of the proposed algorithms and how they scale with dataset size.
   - If applicable, the authors should discuss possible limitations of their approach to address problems of privacy and fairness.
   - While the authors might fear that complete honesty about limitations might be used by reviewers as grounds for rejection, a worse outcome might be that reviewers discover limitations that aren't acknowledged in the paper. The authors should use their best judgment and recognize that individual actions in favor of transparency play an important role in developing norms that preserve the integrity of the community. Reviewers will be specifically instructed to not penalize honesty concerning limitations.

3. **Theory assumptions and proofs**

   Question: For each theoretical result, does the paper provide the full set of assumptions and a complete (and correct) proof?

Answer: [NA]

Justification: Our work does not focus on theoretical proofs.

Guidelines:

- The answer NA means that the paper does not include theoretical results.
- All the theorems, formulas, and proofs in the paper should be numbered and cross-referenced.
- All assumptions should be clearly stated or referenced in the statement of any theorems.
- The proofs can either appear in the main paper or the supplemental material, but if they appear in the supplemental material, the authors are encouraged to provide a short proof sketch to provide intuition.
- Inversely, any informal proof provided in the core of the paper should be complemented by formal proofs provided in appendix or supplemental material.
- Theorems and Lemmas that the proof relies upon should be properly referenced.

4. **Experimental result reproducibility**

   Question: Does the paper fully disclose all the information needed to reproduce the main experimental results of the paper to the extent that it affects the main claims and/or conclusions of the paper (regardless of whether the code and data are provided or not)?

   Answer: [Yes]

   Justification: We provide an anonymous link to the code in the Abstract, enabling experimental result reproduction.

   Guidelines:

   - The answer NA means that the paper does not include experiments.
   - If the paper includes experiments, a No answer to this question will not be perceived well by the reviewers: Making the paper reproducible is important, regardless of whether the code and data are provided or not.
   - If the contribution is a dataset and/or model, the authors should describe the steps taken to make their results reproducible or verifiable.
   - Depending on the contribution, reproducibility can be accomplished in various ways. For example, if the contribution is a novel architecture, describing the architecture fully might suffice, or if the contribution is a specific model and empirical evaluation, it may be necessary to either make it possible for others to replicate the model with the same dataset, or provide access to the model. In general. releasing code and data is often one good way to accomplish this, but reproducibility can also be provided via detailed instructions for how to replicate the results, access to a hosted model (e.g., in the case of a large language model), releasing of a model checkpoint, or other means that are appropriate to the research performed.
   - While NeurIPS does not require releasing code, the conference does require all submissions to provide some reasonable avenue for reproducibility, which may depend on the nature of the contribution. For example
     (a) If the contribution is primarily a new algorithm, the paper should make it clear how to reproduce that algorithm.
     (b) If the contribution is primarily a new model architecture, the paper should describe the architecture clearly and fully.
     (c) If the contribution is a new model (e.g., a large language model), then there should either be a way to access this model for reproducing the results or a way to reproduce the model (e.g., with an open-source dataset or instructions for how to construct the dataset).
     (d) We recognize that reproducibility may be tricky in some cases, in which case authors are welcome to describe the particular way they provide for reproducibility. In the case of closed-source models, it may be that access to the model is limited in some way (e.g., to registered users), but it should be possible for other researchers to have some path to reproducing or verifying the results.

5. **Open access to data and code**

Question: Does the paper provide open access to the data and code, with sufficient instructions to faithfully reproduce the main experimental results, as described in supplemental material?

Answer: [Yes]

Justification: An anonymous link to the code is provided in the Abstract.

Guidelines:

- The answer NA means that paper does not include experiments requiring code.
- Please see the NeurIPS code and data submission guidelines (`https://nips.cc/public/guides/CodeSubmissionPolicy`) for more details.
- While we encourage the release of code and data, we understand that this might not be possible, so "No" is an acceptable answer. Papers cannot be rejected simply for not including code, unless this is central to the contribution (e.g., for a new open-source benchmark).
- The instructions should contain the exact command and environment needed to run to reproduce the results. See the NeurIPS code and data submission guidelines (`https://nips.cc/public/guides/CodeSubmissionPolicy`) for more details.
- The authors should provide instructions on data access and preparation, including how to access the raw data, preprocessed data, intermediate data, and generated data, etc.
- The authors should provide scripts to reproduce all experimental results for the new proposed method and baselines. If only a subset of experiments are reproducible, they should state which ones are omitted from the script and why.
- At submission time, to preserve anonymity, the authors should release anonymized versions (if applicable).
- Providing as much information as possible in supplemental material (appended to the paper) is recommended, but including URLs to data and code is permitted.

6. **Experimental setting/details**

Question: Does the paper specify all the training and test details (e.g., data splits, hyperparameters, how they were chosen, type of optimizer, etc.) necessary to understand the results?

Answer: [Yes]

Justification: We specify our training and test details in the appendix within the Supplementary Material.

Guidelines:

- The answer NA means that the paper does not include experiments.
- The experimental setting should be presented in the core of the paper to a level of detail that is necessary to appreciate the results and make sense of them.
- The full details can be provided either with the code, in appendix, or as supplemental material.

7. **Experiment statistical significance**

Question: Does the paper report error bars suitably and correctly defined or other appropriate information about the statistical significance of the experiments?

Answer: [No]

Justification: Following most previous related work, our experimental results do not include error bars, confidence intervals, or statistical significance tests.

Guidelines:

- The answer NA means that the paper does not include experiments.
- The authors should answer "Yes" if the results are accompanied by error bars, confidence intervals, or statistical significance tests, at least for the experiments that support the main claims of the paper.
- The factors of variability that the error bars are capturing should be clearly stated (for example, train/test split, initialization, random drawing of some parameter, or overall run with given experimental conditions).

- The method for calculating the error bars should be explained (closed form formula, call to a library function, bootstrap, etc.)
- The assumptions made should be given (e.g., Normally distributed errors).
- It should be clear whether the error bar is the standard deviation or the standard error of the mean.
- It is OK to report 1-sigma error bars, but one should state it. The authors should preferably report a 2-sigma error bar than state that they have a 96% CI, if the hypothesis of Normality of errors is not verified.
- For asymmetric distributions, the authors should be careful not to show in tables or figures symmetric error bars that would yield results that are out of range (e.g. negative error rates).
- If error bars are reported in tables or plots, The authors should explain in the text how they were calculated and reference the corresponding figures or tables in the text.

8. **Experiments compute resources**

   Question: For each experiment, does the paper provide sufficient information on the computer resources (type of compute workers, memory, time of execution) needed to reproduce the experiments?

   Answer: [Yes]

   Justification: Compute resource information for reproducing experiments is provided in appendix within the Supplementary Material.

   Guidelines:

   - The answer NA means that the paper does not include experiments.
   - The paper should indicate the type of compute workers CPU or GPU, internal cluster, or cloud provider, including relevant memory and storage.
   - The paper should provide the amount of compute required for each of the individual experimental runs as well as estimate the total compute.
   - The paper should disclose whether the full research project required more compute than the experiments reported in the paper (e.g., preliminary or failed experiments that didn't make it into the paper).

9. **Code of ethics**

   Question: Does the research conducted in the paper conform, in every respect, with the NeurIPS Code of Ethics `https://neurips.cc/public/EthicsGuidelines`?

   Answer: [Yes]

   Justification: Our research does not violate any NeurIPS Code of Ethics.

   Guidelines:

   - The answer NA means that the authors have not reviewed the NeurIPS Code of Ethics.
   - If the authors answer No, they should explain the special circumstances that require a deviation from the Code of Ethics.
   - The authors should make sure to preserve anonymity (e.g., if there is a special consideration due to laws or regulations in their jurisdiction).

10. **Broader impacts**

    Question: Does the paper discuss both potential positive societal impacts and negative societal impacts of the work performed?

    Answer: [Yes]

    Justification: We discuss the broader impacts of our work in the appendix within the Supplementary Material.

    Guidelines:

    - The answer NA means that there is no societal impact of the work performed.
    - If the authors answer NA or No, they should explain why their work has no societal impact or why the paper does not address societal impact.

- Examples of negative societal impacts include potential malicious or unintended uses (e.g., disinformation, generating fake profiles, surveillance), fairness considerations (e.g., deployment of technologies that could make decisions that unfairly impact specific groups), privacy considerations, and security considerations.
- The conference expects that many papers will be foundational research and not tied to particular applications, let alone deployments. However, if there is a direct path to any negative applications, the authors should point it out. For example, it is legitimate to point out that an improvement in the quality of generative models could be used to generate deepfakes for disinformation. On the other hand, it is not needed to point out that a generic algorithm for optimizing neural networks could enable people to train models that generate Deepfakes faster.
- The authors should consider possible harms that could arise when the technology is being used as intended and functioning correctly, harms that could arise when the technology is being used as intended but gives incorrect results, and harms following from (intentional or unintentional) misuse of the technology.
- If there are negative societal impacts, the authors could also discuss possible mitigation strategies (e.g., gated release of models, providing defenses in addition to attacks, mechanisms for monitoring misuse, mechanisms to monitor how a system learns from feedback over time, improving the efficiency and accessibility of ML).

11. **Safeguards**

    Question: Does the paper describe safeguards that have been put in place for responsible release of data or models that have a high risk for misuse (e.g., pretrained language models, image generators, or scraped datasets)?

    Answer: [Yes]

    Justification: We discuss the safeguards in the appendix within the Supplementary Material.

    Guidelines:

    - The answer NA means that the paper poses no such risks.
    - Released models that have a high risk for misuse or dual-use should be released with necessary safeguards to allow for controlled use of the model, for example by requiring that users adhere to usage guidelines or restrictions to access the model or implementing safety filters.
    - Datasets that have been scraped from the Internet could pose safety risks. The authors should describe how they avoided releasing unsafe images.
    - We recognize that providing effective safeguards is challenging, and many papers do not require this, but we encourage authors to take this into account and make a best faith effort.

12. **Licenses for existing assets**

    Question: Are the creators or original owners of assets (e.g., code, data, models), used in the paper, properly credited and are the license and terms of use explicitly mentioned and properly respected?

    Answer: [Yes]

    Justification: We cite all referenced works and adhere to their licenses and usage terms.

    Guidelines:

    - The answer NA means that the paper does not use existing assets.
    - The authors should cite the original paper that produced the code package or dataset.
    - The authors should state which version of the asset is used and, if possible, include a URL.
    - The name of the license (e.g., CC-BY 4.0) should be included for each asset.
    - For scraped data from a particular source (e.g., website), the copyright and terms of service of that source should be provided.
    - If assets are released, the license, copyright information, and terms of use in the package should be provided. For popular datasets, `paperswithcode.com/datasets` has curated licenses for some datasets. Their licensing guide can help determine the license of a dataset.

- For existing datasets that are re-packaged, both the original license and the license of the derived asset (if it has changed) should be provided.
- If this information is not available online, the authors are encouraged to reach out to the asset's creators.

13. **New assets**

    Question: Are new assets introduced in the paper well documented and is the documentation provided alongside the assets?

    Answer: [NA]

    Justification: The paper does not release new assets.

    Guidelines:

    - The answer NA means that the paper does not release new assets.
    - Researchers should communicate the details of the dataset/code/model as part of their submissions via structured templates. This includes details about training, license, limitations, etc.
    - The paper should discuss whether and how consent was obtained from people whose asset is used.
    - At submission time, remember to anonymize your assets (if applicable). You can either create an anonymized URL or include an anonymized zip file.

14. **Crowdsourcing and research with human subjects**

    Question: For crowdsourcing experiments and research with human subjects, does the paper include the full text of instructions given to participants and screenshots, if applicable, as well as details about compensation (if any)?

    Answer: [NA]

    Justification: The paper does not involve crowdsourcing nor research with human subjects.

    Guidelines:

    - The answer NA means that the paper does not involve crowdsourcing nor research with human subjects.
    - Including this information in the supplemental material is fine, but if the main contribution of the paper involves human subjects, then as much detail as possible should be included in the main paper.
    - According to the NeurIPS Code of Ethics, workers involved in data collection, curation, or other labor should be paid at least the minimum wage in the country of the data collector.

15. **Institutional review board (IRB) approvals or equivalent for research with human subjects**

    Question: Does the paper describe potential risks incurred by study participants, whether such risks were disclosed to the subjects, and whether Institutional Review Board (IRB) approvals (or an equivalent approval/review based on the requirements of your country or institution) were obtained?

    Answer: [NA]

    Justification: The paper does not involve crowdsourcing nor research with human subjects.

    Guidelines:

    - The answer NA means that the paper does not involve crowdsourcing nor research with human subjects.
    - Depending on the country in which research is conducted, IRB approval (or equivalent) may be required for any human subjects research. If you obtained IRB approval, you should clearly state this in the paper.
    - We recognize that the procedures for this may vary significantly between institutions and locations, and we expect authors to adhere to the NeurIPS Code of Ethics and the guidelines for their institution.
    - For initial submissions, do not include any information that would break anonymity (if applicable), such as the institution conducting the review.

16. **Declaration of LLM usage**

    Question: Does the paper describe the usage of LLMs if it is an important, original, or non-standard component of the core methods in this research? Note that if the LLM is used only for writing, editing, or formatting purposes and does not impact the core methodology, scientific rigorousness, or originality of the research, declaration is not required.

    Answer: [NA]

    Justification: The core method development in this research does not involve LLMs as any important, original, or non-standard components.

    Guidelines:

    - The answer NA means that the core method development in this research does not involve LLMs as any important, original, or non-standard components.
    - Please refer to our LLM policy (`https://neurips.cc/Conferences/2025/LLM`) for what should or should not be described.

Appendix Overview

The anonymous project of our paper is in `https://janus-pro-r1.github.io`. In this supplementary material, we present:

- Preliminary on GRPO in Section A.
- Implementation Details in Section B.
- Evaluation Details in Section C.
- More Experimental Results in Section D.
- Limitation, Future Work, Broader Impacts and Safeguards in Section E.

A Preliminary on GRPO

Recently, reinforcement learning [16, 27] has emerged as the primary method for unlocking the reasoning capabilities of LLMs. The study by [45] introduces the Group Relative Policy Optimization (GRPO) framework. GRPO enhances Proximal Policy Optimization (PPO) [44] by eliminating the value function and estimating the advantages in a group-relative manner. Specifically, given the input instruction q, the old policy $\pi_{\theta_{old}}$ first samples a group of G individual responses as the response group $\mathcal{G} = \{o_i^1\}_{i=1}^G$. We input each response with the group into the reward function to obtain the individual reward $\mathtt{R}_i$. We then calculate the advantages $\{A_i\}_{i=1}^G$, where each A_i measures the relative quality of output compared to the average reward:

$$A_i = \frac{\mathtt{R}_i - \text{mean}\big(\{\mathtt{R}_i\}_{i=1}^G\big)}{\text{std}\big(\{\mathtt{R}_i\}_{i=1}^G\big)} \tag{4}$$

The GRPO method employs a clipped objective function, similar to PPO, and introduces a KL divergence constraint that compares the current policy π_θ with the reference model $\pi_{\theta_{ref}}$ into the loss function, as follows:

$$\mathcal{J}(\theta) = \mathbb{E}_{\substack{(q,a)\sim\mathcal{D} \\ \{o_i\}_{i=1}^G \sim \pi_{\theta_{\text{old}}}(\cdot|q)}} \left[\frac{1}{\sum_{i=1}^G |o_i|} \sum_{i=1}^{G} \sum_{j=1}^{|o_i|} \left(\min\Big(\rho_{i,j} A_i, \text{clip}\Big(\rho_{i,j}, 1-\varepsilon, 1+\varepsilon\Big) A_i\Big) - \beta D_{\text{KL}}(\pi_\theta || \pi_{\theta_{ref}}) \right) \right], \tag{5}$$

where $D_{\text{KL}}(\pi_\theta||\pi_{\theta_{ref}}) = \frac{\pi_{ref}}{\pi} - \log\frac{\pi_{ref}}{\pi} - 1$ is the the KL divergence to maintain training stability. And $\rho_{i,j} = \frac{\pi_\theta(o_{i,j}|q,o_{i,<j})}{\pi_{\theta_{\text{old}}}(o_{i,j}|q,o_{i,<j})}$ is the ratio between the probabilities of π_θ and $\pi_{\theta_{\text{old}}}$ for outputting the current token.

B Implementation Details

B.1 Supervised Fine-Tuning

For SFT, we construct an image-text collection $\mathcal{C} = \{\mathcal{P}_i : \{(\mathcal{I}_i^j, \mathcal{S}_i^j, \mathcal{R}_i^j)\}_{j=1}^M\}_{i=1}^N$ as the supervised training data, where each prompt $\mathcal{P}$ corresponds to M images $\{\mathcal{I}_i^j\}_{j=1}^M$. For each image-text pair, there is an associated semantic consistency score $\mathcal{S} \in [0, 1]$ and a detailed reason $\mathcal{R}$ for semantic matching ($\mathcal{S} >$ 0.5) or non-matching ($\mathcal{S} <$ 0.5), where $S^0 > S^1 > ... > S^M$. Specifically, we first develop a set of seed prompts and leverage the Qwen [1] model to expand them into a total of $N = 200,000$ prompts, covering various types (color, shape, spatial, etc.) with $80,000$ short captions and $120,000$ long captions. For each prompt, we employ the FLUX [23] and Janus-Pro-1B/7B [5] models for text-to-image generation, producing $M = 18$ images per prompt. Subsequently, we utilize the InternVL2.5-26B [6] model as the evaluation model, instructing it with the question of whether the image and text are semantically consistent with the following prompt "`Does this image match the description? Please directly respond with yes or no`". We record the probability to answer "Yes" as P_{Yes} and "No" as P_{No}, with $\mathcal{S} = P_{\text{Yes}}/(P_{\text{Yes}} + P_{\text{No}})$. And for each prompt, we sort its associated M images based on their semantic consistency scores in descending order. In addition, to construct the long captions, we first collect some short captions. Subsequently, we prompt Qwen to expand these short captions using the following prompt:

Please generate the long prompt version of the short one according to the given examples. Long prompt version should consist of 3 to 5 sentences. Long prompt version must sepcify the color, shape, texture or spatial relation of the included objects. DO NOT generate sentences that describe any atmosphere.
Short: `Case1-Short`.
Long: `Case1-Long`.
Short: `Case1-Short`.
Long: `Case1-Long`.
Short: `Caption-Shot`.

During supervised fine-tuning, we set $t = 3$ for Task-II and $t = 2$ for Task-III, which means that we allow the MLLMs to generate up to three images (one text-to-image generation and two image regenerations) given a prompt. For mixed training, we set the mixing ratios for Task-I, Task-II, and Task-III as 0.2, 0.3, and 0.5, respectively. More training hyperparameters are detailed in Table5.

Furthermore, given that Janus-Pro integrates two distinct types of image encoders, the understanding encoder is specifically the SIGLIP encoder [60], while the generation encoder is the VQ tokenizer from [46]. For all input images in Task-II, the understanding encoder is employed to encode the input visual embeddings, whereas for all input images in Task-III, the generation encoder is used to encode the input visual embeddings. Additionally, for Task-I and Task-III, each sample's input prompt $\mathcal{P}$ has a 10% probability of being replaced with `[PAD]` tokens.

B.2 Reward Calculation

The overall design philosophy of our reward model is to leverage QA-based visual comprehension [6, 25, 36, 24, 42, 8, 30, 29] models, which will return a consistency score $\mathtt{R}^{QA}(\cdot) \in [0, 1]$ for each text-image pair, to assess the accuracy of the generated image and the MLLM's self-evaluation. And we provide incentives for the final output images along with their preceding reasoning chains, incorporating **bi-level reward scores**: visual generation reward $\mathtt{R}^{Gen}$ and visual comprehension reward $\mathtt{R}^{Comp}$. Assume that we permit the MLLM to perform up to a maximum of T-round image generations and the MLLM determines that it has correctly generated the image in the K-th round (resulting in a total of K images $\{\mathcal{I}^i\}_{i=1}^{K}$, $T \geq K$), we have: **(1) The generation reward** $\mathtt{R}^{Gen} = \sum_{i=1}^{K-1} \mathtt{R}^{QA}(\mathcal{I}^i) + (T - K + 1) \times \mathtt{R}^{QA}(\mathcal{I}^K)$. The K-th image is assigned a potentially larger weight because it represents the final output with higher importance. **(2) The comprehension reward** $\mathtt{R}^{Comp} = \sum_{i=1}^{K} \left(\mathbf{1} - |\mathtt{R}^{QA}(\mathcal{I}^i) - \mathtt{SE}(\mathcal{I}^i)|\right) \times T/K$, where $\mathtt{SE}(\mathcal{I}) = 0$ or 1 is the self-assessment on whether the generated image is semantically aligned with the text.

To calculate the consistency score, we leverage InternVL2.5-26B [6] as the reward model to provide appropriate incentives, which will return a consistency score $\mathtt{R}_{\mathcal{I}} \in [0, 1]$ for each text-image pair. Specifically, for short prompts, we directly the MLLM with the question "`Does this image match the description? Please directly respond with yes or no`". We record the probability of the model responding with "Yes" as P_{yes} and "No" as P_{no}, with the consistency score calculated as $\mathtt{R}^{QA} = P_{yes}/(P_{yes} + P_{no})$.

For long prompts, inspired by [7], we first decompose the prompt into semantic tuples (*e.g.*, attributes and spatial relations) and then generate corresponding yes-or-no questions (*e.g.*, "Is the dog red?"). The reward model is then tasked with performing a VQA task for the prompt and the generated image, returning a score between 0 and 1 for each question in the same manner. The consistency score is obtained by averaging the evaluations of the reward model across multiple questions for a given prompt.

B.3 Reinforcement Learning

During RL training, we use Janus-Pro-SFT as the backbone model and set the batch size to 128, the group size to 7, and β to 0.05. All parameters are tunable. We totally conduct 3000 iterations of post-training optimization. We find that the learning rate is crucial: a learning rate that is too small results in insignificant performance gains, while a learning rate that is too large leads to unstable training. To address this, we design a combined Linear + Cosine learning rate scheduler. The learning rate quickly drops linearly from a peak value to a lower "convert learning rate" at a "convert step",

Table 5: The detailed training hyper-parameters of SFT and RL for both text-to-image and image editing tasks.

Hyper-parameters	**SFT for T2I**	**RL for T2I**	**SFT for Image Editing**	**RL for Image Editing**
Optimizer	AdamW	AdamW	AdamW	AdamW
Optimizer param.	$\beta_1 = 0.9, \beta_2 = 0.95, \epsilon = \text{1e}{-6}$		$\beta_1 = 0.9, \beta_2 = 0.95, \epsilon = \text{1e}{-6}$	
Peak LR	2.0e-5	6.0e-6	2.0e-5	1.0e-5
Convert LR	-	2.0e-6	-	2.0e-6
Convert step	-	400	-	300
Min LR	2.0e-7	2.0e-7	2.0e-7	2.0e-7
LR scheduler	Cosine	Linear+Cosine	Cosine	Linear+Cosine
Batch size	128	128	128	128
Group size	-	7	-	8
β	-	0.05	-	0.05
Training Steps	50K	3K	40K	2.2K
Warmup Steps	1000	100	1000	100
Weight decay	0.05	0.05	0.05	0.05
Gradient clipping	1.0	1.0	1.0	1.0
Numerical precision	bfloat16	bfloat16	bfloat16	bfloat16
Resource Usage	8 NVIDIA A800	32 NVIDIA A800	8 NVIDIA A800	32 NVIDIA A800

and then gradually decreases along a cosine curve. However, we still encounter some instability during training, indicated by a downward trend in the reward curve. To address this, we adopt the following measures:

(1) When the reward curve dropped sharply, we reduce the learning rate to half or two-thirds of its current value and resume the training;

(2) When the reward curve declines gradually, it indicates that the KL divergence constraint imposed by a less capable reference model is limiting further improvement of the current model. To address this, we propose two measures: If the optimization steps applied to the current model relative to the reference model are small, we reduce the KL divergence constraint weight by setting a smaller β value and then resume training. Otherwise, we update the reference model to the current model and then resume the training.

The detailed hyperparameters for training are shown in Table 5.

B.4 Inference

Janus-Pro-R1 can generate both text and images with two separate MLLM heads: an image head for predicting image tokens and a text head for predicting text tokens. We transform the text-to-image generation into an introspective process [41, 37, 38]. During inference, when provided with a prompt, the model initially engages the image head to perform an autoregressive prediction of 576 visual tokens to generate the first image. Subsequently, it switches to the text head to assess whether the generated image aligns with the semantic of the prompt and to predict a relevant reason. If the model determines that the image is consistent with the prompt, the inference is terminated, and the generated image is output. Conversely, if the model deems the image inconsistent, it switches back to the image head to predict another 576 visual tokens for a new image generation attempt. The model then reverts to the text head to reassess the semantic alignment and predict a reason. This cycle of switching between the image and text heads continues iteratively. Of course, to prevent infinite image generation, the model is constrained to generate a maximum of 3 images for each inference.

Furthermore, considering that Janus-Pro incorporates two types of image encoders, during image generation with CoT, we select the image encoder in the following manner: when the model leverages the text head to output text (Task-II), all preceding images are encoded using the understanding encoder. Conversely, when the model leverages the image head to output image tokens (Task-III), all preceding images are encoded using the generation encoder.

Moreover, we set $topk = 50$ for text token sampling and $topk = 4096$ for visual token sampling. Besides, for text-to-image generation (Task-I) and image regeneration (Task-III), during inference we use classifier-free guidance on the logits for autoregressive sampling in a manner similar to [39, 52, 28]. We set the guidance scale to 5.0. It is important to note that during both text-to-image generation and image regeneration, we only mask the input text prompt $\mathcal{P}$ with `[PAD]` tokens to facilitate classifier-free guidance.

B.5 Implementation Details of Image Editing

Supervised Fine-Tuning. We first collect image editing training data from [62] and [59]. Given the suboptimal quality of existing image editing datasets, we first conduct a data cleaning process on the training data. With InternVL2.5-26B [6] as the evaluation MLLM, we provide it with before-and-after-editing images along with editing instructions, and then pose the following two questions for each image editing training sample $(\mathcal{I}^c, \mathcal{P}^{ins}, \mathcal{I}^{out})$ inspired by [15]:

(1) Instruction Following Question: `Does the edited image follow the instruction? Please directly respond with yes or no.`

(2) Detail Preserving Question: `Are the non-edited areas of the edited image consistent with the original image? Please directly respond with yes or no.`

For each question, we recorded the probability of the evaluation MLLM responding with “Yes” as P^{flw}_{yes} or P^{psv}_{yes} and P^{flw}_{no} or P^{psv}_{no}, with following score calculated as $S^{flw}(\mathcal{I}^c, \mathcal{P}^{ins}, \mathcal{I}^{out}) = P^{flw}_{yes}/(P^{flw}_{yes} + P^{flw}_{no})$ and preserving score as $S^{psv}(\mathcal{I}^c, \mathcal{P}^{ins}, \mathcal{I}^{out}) = P^{psv}_{yes}/(P^{psv}_{yes} + P^{psv}_{no})$. For each sample, we incorporate it into the training dataset only if both $S^{psv}(\mathcal{I}^c, \mathcal{P}^{ins}, \mathcal{I}^{out}) \geq 0.7$ and $S^{flw}(\mathcal{I}^c, \mathcal{P}^{ins}, \mathcal{I}^{out}) \geq 0.7$. Furthermore, during SFT, each sample's instruction has a 10% probability of being dropped out as `[PAD]` tokens. And we detail the training hyper-parameters for image editing SFT in Table 5.

Reinforcement Learning. During reinforcement learning, we no longer provide ground-truth edited images. Instead, we allow the model to autonomously predict the edited images based on the input images and instructions, only providing proper incentives according to the GRPO algorithm. We still leverage InternVL2.5-26B [6] as the reward model and design two QA-based rewards: (1) Following score $\texttt{R}^{flw} \in [0, 1]$ measures whether the model accurately follows the editing request; (2) Preserving score $\texttt{R}^{psv} \in [0, 1]$ indicates how well the model preserves details that are not intended to be changed. The calculation methods for these two scores are identical to those described in the preceding paragraph for computing the following score and the preserving score. And the final reward is calculated as $\texttt{R}^{edit} = 0.5 * \texttt{R}^{flw} + \texttt{R}^{psv}$. , where $\texttt{R}_{flw}$ is assigned with a relatively low weight as we prioritize enhancing the model's ability to maintain local fidelity. And we find that a smaller weight for $\texttt{R}_{flw}$ tends to lead the model to output the pre-edited image directly in order to achieve a higher overall reward value. Furthermore, we set the group size to 8 and the batch size to 128. The trick that enables stable RL training is similar to that described in Appendix B.3. We provide additional details of the hyperparameters for image editing RL in Table 5.

Inference. During inference, the input images are encoded using the generation encoder. We set $topk = 4096$ and also employ classifier-free guidance on the logits for autoregressive sampling with the guidance scale of 4.0. We only mask the input text instruction P^{inc} with `[PAD]` tokens to facilitate classifier-free guidance without masking the input image.

C Evaluation Details

C.1 Baseline Methods

For text-to-image generation tasks, we compare Janus-Pro-R1 with diffusion-based and MLLM-based methods, as well as MLLMs incorporating CoT into image generation. The diffusion-based baselines include PixArt-alpha [4], DALL-E3 [2], SD3 [9], FLUX.1-dev [23], Sana-1.5 [57], and Janus-Flow [31]. The MLLM-based baselines include Show-o [58], SEED-X [12], Emu-3 [52], DDT-LLaMA [39], VARGPTv1.1 [64], Infinity [18], Janus-Pro [5], GPT-4o [34]. The MLLM+CoT baselines include Show-o+PARM [17], MINT [53], GOT [10], T2I-R1 [21]. To ensure a fair comparison, for the last category of baselines, we report results without inference-time scaling.

For image editing tasks, we compare Janus-Pro-R1 with instruction-based large-scale training methods, including InstructPix2Pix [3], MagicBrush [61], InstructDiffusion [13], MGIE [11], Seed-X-Edit [12], and EditAR [32].

C.2 Evaluation Benchmarks

We conduct zero-shot evaluation on 3 existing text-to-image benchmarks: GenEval [14], T2I-CompBench [20], and DPG-Bench [19]. GenEval contains 6 different subtasks of varying difficulty requiring various compositional skills, including `single object` (SingObj), `single object` (TwoObj), `counting`, `colors`, `position`, `color binding` (ColorAttri). And we adopt the metric proposed by [14] for evaluation. Each subtask is scored independently, and the overall score is calculated as the average of all six subtask scores. The T2I-CompBench encompasses three subtasks following [52]: `color`, `shape`, `texture`. Building on prior research, we employ the Blip-VQA score [26] as the evaluation metric. For DPG-Bench, we follow the metrics proposed in [19] to conduct the evaluation.

For the image editing task, we conduct zero-shot evaluation on Pie-bench [22] with 700 examples, covering 10 editing types. Our method uses the source image and editing instructions to predict the target edit. Both reconstruction and text-to-image alignment are evaluated as in [22] with the annotated foreground masks, with structure distance and background preservation metrics reflecting fidelity preservation, while CLIP similarity is used for editability evaluation.

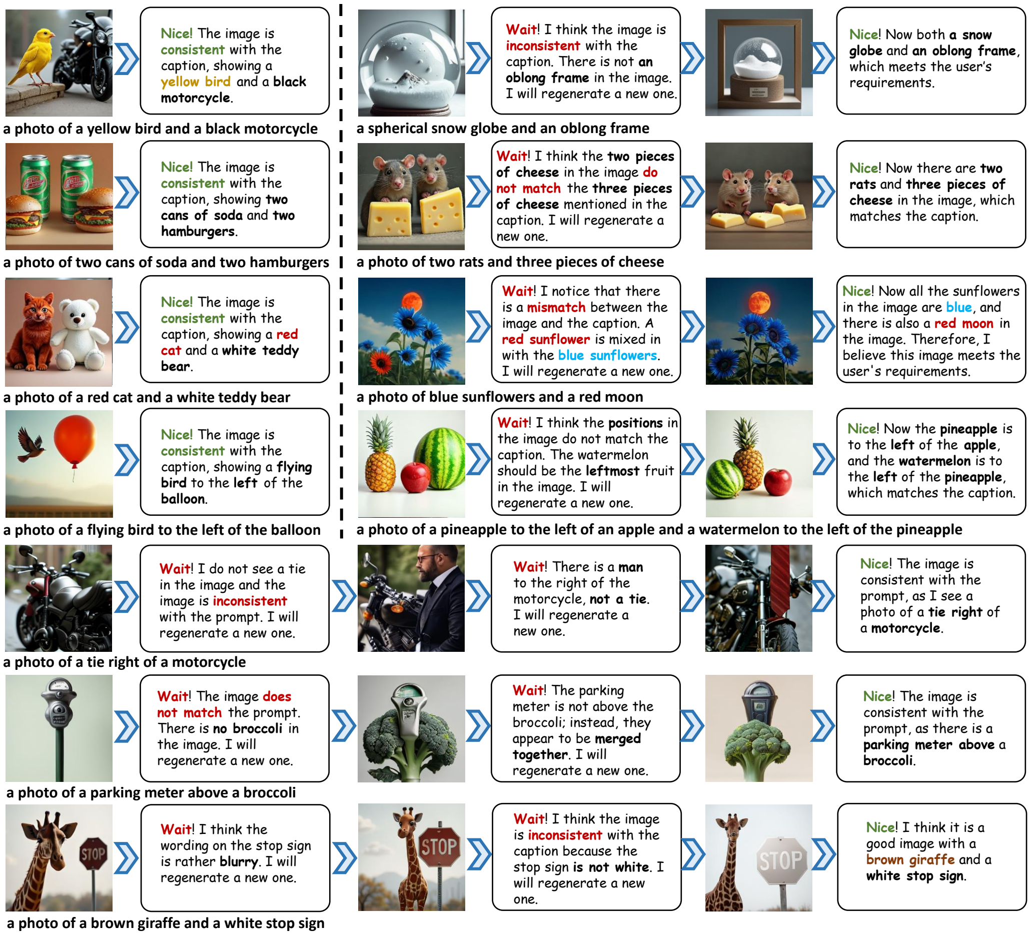
Nice! The image is consistent with the caption, showing a yellow bird and a black motorcycle.
a photo of a yellow bird and a black motorcycle
Wait! I think the image is inconsistent with the caption. There is not an oblong frame in the image. I will regenerate a new one.
Nice! Now both a snow globe and an oblong frame, which meets the user's requirements.
a spherical snow globe and an oblong frame
Nice! The image is consistent with the caption, showing two cans of soda and two hamburgers.
a photo of two cans of soda and two hamburgers
Wait! I think the two pieces of cheese in the image do not match the three pieces of cheese mentioned in the caption. I will regenerate a new one.
Nice! Now there are two rats and three pieces of cheese in the image, which matches the caption.
a photo of two rats and three pieces of cheese
Nice! The image is consistent with the caption, showing a red cat and a white teddy bear.
a photo of a red cat and a white teddy bear
Wait! I notice that there is a mismatch between the image and the caption. A red sunflower is mixed in with the blue sunflowers. I will regenerate a new one.
Nice! Now all the sunflowers in the image are blue, and there is also a red moon in the image. Therefore, I believe this image meets the user's requirements.
a photo of blue sunflowers and a red moon
Nice! The image is consistent with the caption, showing a flying bird to the left of the balloon.
a photo of a flying bird to the left of the balloon
Wait! I think the positions in the image do not match the caption. The watermelon should be the leftmost fruit in the image. I will regenerate a new one.
Nice! Now the pineapple is to the left of the apple, and the watermelon is to the left of the pineapple, which matches the caption.
a photo of a pineapple to the left of an apple and a watermelon to the left of the pineapple
Wait! I do not see a tie in the image and the image is inconsistent with the prompt. I will regenerate a new one.
Wait! There is a man to the right of the motorcycle, not a tie. I will regenerate a new one.
Nice! The image is consistent with the prompt, as I see a photo of a tie right of a motorcycle.
a photo of a tie right of a motorcycle
Wait! The image does not match the prompt. There is no broccoli in the image. I will regenerate a new one.
Wait! The parking meter is not above the broccoli; instead, they appear to be merged together. I will regenerate a new one.
Nice! The image is consistent with the prompt, as there is a parking meter above a broccoli.
a photo of a parking meter above a broccoli
Wait! I think the wording on the stop sign is rather blurry. I will regenerate a new one.
Wait! I think the image is inconsistent with the caption because the stop sign is not white. I will regenerate a new one.
Nice! I think it is a good image with a brown giraffe and a white stop sign.
a photo of a brown giraffe and a white stop sign
STOP

Figure 7: More qualitative examples of introspective text-to-image generation that triggers Aha moments.

D More Experimental Results

In Figure 7, we present more qualitative examples of Janus-Pro-R1 to trigger Aha moments within its reasoning chains to generate superior images. Our model could leverage its visual comprehension capabilities to accurately identify the issues in its initial-generated images, then unleash the visual generation capabilities to output a more accurate image.

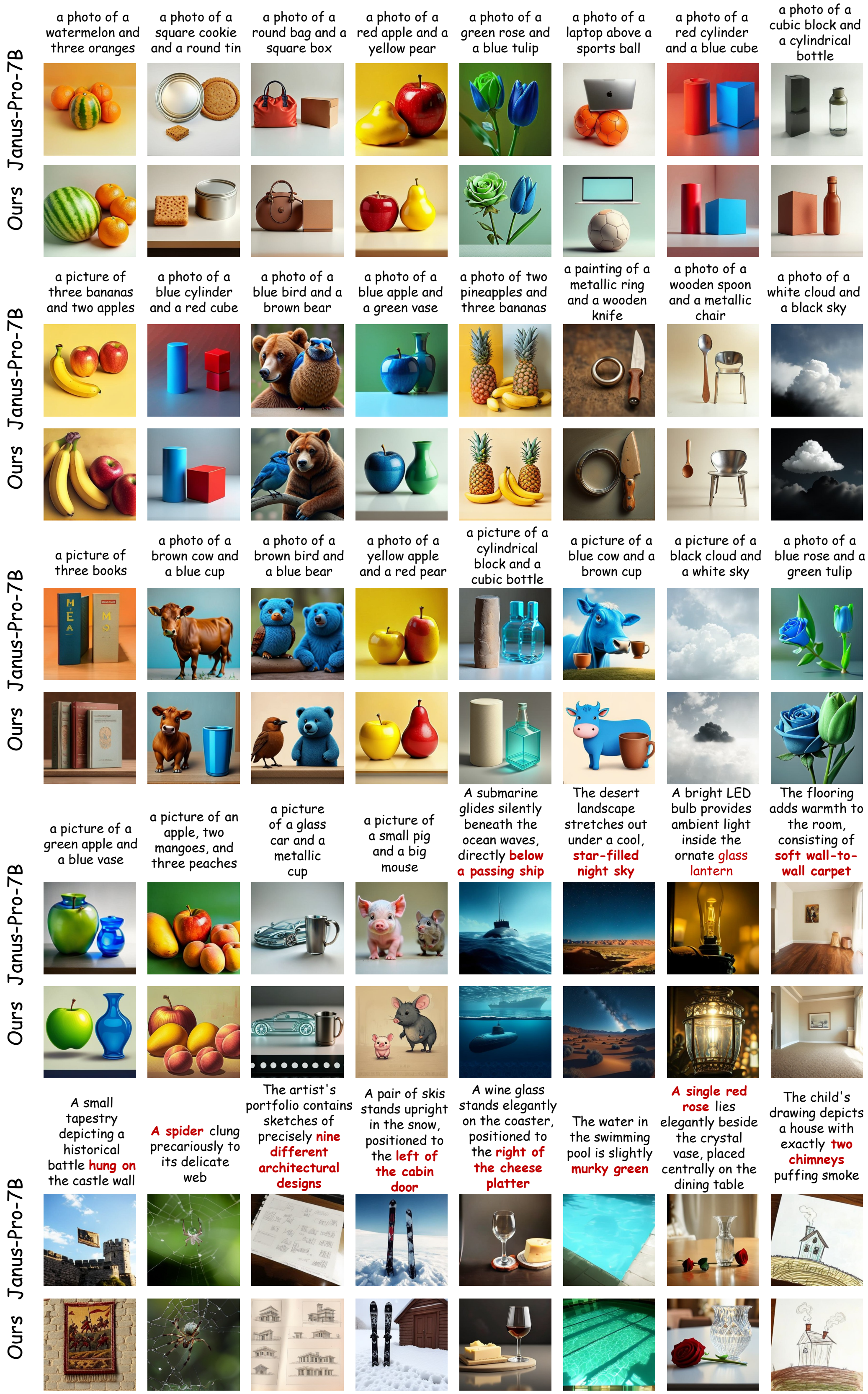
a photo of a watermelon and three oranges
a photo of a square cookie and a round tin
a photo of a round bag and a square box
a photo of a red apple and a yellow pear
a photo of a green rose and a blue tulip
a photo of a laptop above a sports ball
a photo of a red cylinder and a blue cube
a photo of a cubic block and a cylindrical bottle
Janus-Pro-7B
Ours
a picture of three bananas and two apples
a photo of a blue cylinder and a red cube
a photo of a blue bird and a brown bear
a photo of a blue apple and a green vase
a photo of two pineapples and three bananas
a painting of a metallic ring and a wooden knife
a photo of a wooden spoon and a metallic chair
a photo of a white cloud and a black sky
Janus-Pro-7B
Ours
a picture of three books
a photo of a brown cow and a blue cup
a photo of a brown bird and a blue bear
a photo of a yellow apple and a red pear
a picture of a cylindrical block and a cubic bottle
a picture of a blue cow and a brown cup
a picture of a black cloud and a white sky
a photo of a blue rose and a green tulip
Janus-Pro-7B
Ours
a picture of a green apple and a blue vase
a picture of an apple, two mangoes, and three peaches
a picture of a glass car and a metallic cup
a picture of a small pig and a big mouse
A submarine glides silently beneath the ocean waves, directly below a passing ship
The desert landscape stretches out under a cool, star-filled night sky
A bright LED bulb provides ambient light inside the ornate glass lantern
The flooring adds warmth to the room, consisting of soft wall-to-wall carpet
Janus-Pro-7B
Ours
A small tapestry depicting a historical battle hung on the castle wall
A spider clung precariously to its delicate web
The artist's portfolio contains sketches of precisely nine different architectural designs
A pair of skis stands upright in the snow, positioned to the left of the cabin door
A wine glass stands elegantly on the coaster, positioned to the right of the cheese platter
The water in the swimming pool is slightly murky green
A single red rose lies elegantly beside the crystal vase, placed centrally on the dining table
The child's drawing depicts a house with exactly two chimneys puffing smoke
Janus-Pro-7B
Ours

Figure 8: Qualitative Comparisons between Janus-Pro-7B and our Janus-Pro-R1-7B on the final generated image for text-to-image generation task.

Figure 8 presents a direct qualitative comparison between Janus-Pro-7B and our Janus-Pro-R1-7B on the text-to-image generation task, with both short and long captions. It can be observed that compared to Janus-Pro-7B, after unlocking the Aha moments with CoT via a two-stage training paradigm, our model not only generates images that are more semantically aligned with the text but also achieves higher aesthetic quality.

E Limitation, Future Work, Broader Impacts and Safeguards

Limitations. **Firstly,** in the text-to-image generation task, our constructed prompt data contains relatively few instances related to counting. This directly results in our model's counting metric on the Geneval dataset lagging behind SOTA models. To address this issue, we will further specifically construct a set of counting-related data to enhance the corresponding capabilities for counting-related prompts. **Secondly,** in the image editing task, although the existing datasets meet the requirements for image editing, many of the data samples have poor aesthetic appeal. This leads to some edited images lacking in aesthetic quality. To improve this, we plan to use GPT-4o to create a set of high-aesthetic image editing data in the future to enhance the natural appearance of the edited images.

Future Work. In the future, we plan to harness more substantial computational resources to design increasingly complex interleaved text-image generation tasks. We are convinced that reinforcement learning has the potential to bring about revolutionary changes to unified visual comprehension and generation, thereby significantly raising the upper limit of such unification. To this end, we will cover a broader range of visual understanding and visual generation tasks, seamlessly integrate these two capabilities, and tackle the open-ended interleaved text-image generation problem. Ultimately, we hope to transform MLLMs into a more intelligent multimodal dialogue system.

Broader Impacts. This study does not raise any ethical concerns. The research does not involve subjective assessments or the use of private data. Only publicly available datasets are utilized for experimentation.

Safeguards. A major societal concern with this technology lies in its potential for misuse, particularly in fabricating unauthorized images that could lead to misinformation, privacy breaches, and other damaging consequences. To counter these threats, it is crucial to develop strong ethical standards and implement ongoing surveillance.